

UNIVERSITÀ
DI PAVIA



IUSS

UNIVERSITY OF PAVIA
FACULTY OF ENGINEERING

UNIVERSITY SCHOOL OF ADVANCED STUDIES - IUSS PAVIA

Exploring benefit cost analysis to support earthquake risk mitigation in Central America

A Thesis Submitted in Partial Fulfilment of the Requirements
for the Degree of Master of Science (Laurea Magistrale) in

Civil Engineering for the Mitigation of Risk from Natural Hazards

by

Maria Camila Hoyos Ramirez
Supervisor: Giammaria Gabbianelli
Co-Supervisor: Bryan Chalarca Echeverri

September 2026

ABSTRACT

This thesis develops a comprehensive methodology for conducting benefit–cost analyses aimed at identifying optimal seismic retrofitting strategies for the two most vulnerable building typologies in Central America: unreinforced masonry and adobe structures. The approach incorporates both direct losses associated with structural damage and indirect losses related to injuries and fatalities. A detailed review of existing retrofitting techniques was carried out, resulting in a database that compiles implementation costs and expected structural improvement to performance in terms of strength, stiffness, and ductility. Using characteristics of representative vulnerable buildings—both in their original and retrofitted configurations—capacity curves were generated through Non-Linear Time History Analyses (NLTHA) applied to Single Degree of Freedom (SDOF) oscillators. These curves served as the basis for deriving updated fragility functions and for estimating future seismic losses. Probabilistic seismic risk assessments were then performed for each building class, comparing baseline conditions with retrofitted alternatives. Average annual losses were calculated to quantify the expected annual savings associated with each intervention, and benefit–cost ratios were obtained by relating these savings to the corresponding retrofitting costs. The results indicate that, under a 50-year evaluation period and a 4% discount rate, retrofitting these building typologies can be economically viable, particularly in regions along the western coast of Central America where seismic hazard is highest.

Keywords: seismic risk; benefit-cost analysis; retrofitting techniques; fragility curves; adobe; URM.

TABLE OF CONTENTS

ABSTRACT iii
TABLE OF CONTENTS v
LIST OF FIGURES vii
LIST OF TABLES ix
LIST OF SYMBOLS xi
1. INTRODUCTION 1
2. CHARACTERIZATION OF RESIDENTIAL BUILDING STOCK IN THE REGION 5
3. SELECTION OF RETROFITTING TECHNIQUES 9
3.1 RETROFITTING TECHNIQUES FOR UNREINFORCED MASONRY BUILDINGS 9
3.1.1 Surface Treatment – Ferrocement 12
3.1.2 External fibre reinforced polymers (FRP) 13
3.1.3 Polymer and steel bands 13
3.2 RETROFITTING TECHNIQUES FOR ADOBE BUILDINGS 14
3.2.1 External Steel Mesh 16
3.2.2 External Synthetic Mesh 17
3.2.3 External near-surface mounted (NSM) steel rebars 17
3.2.4 Timber confinement 17
4. VULNERABILITY ASSESSMENT OF RETROFFITED CASES 19
4.1 QUANTIFICATION OF UNCERTAINTY IN THE VMTK 20
4.2 DEFINITION OF THE CAPACITY CURVES 22
4.2.1 In-plane behaviour 22
4.2.2 Out-of-plane behaviour 22
4.3 DERIVATION OF FRAGILITY FUNCTIONS 25
4.4 DERIVATION OF VULNERABILITY FUNCTIONS 29
5. BENEFIT COST ANALYSIS 33

6. CONCLUSIONS 39
REFERENCES 41

LIST OF FIGURES

Figure 2.1. Distribution of the number of buildings in Central America (CR: Reinforced concrete, CR+PC: Precast concrete, MCF: Confined masonry, MR: Reinforced masonry, MUR: Unreinforced masonry, MUR+ADO: Adobe, MUR+ST: Stone masonry, UNK: Unknown, W+WBB: Bamboo wood, W'+WLI: Light wood, W+WS: Strong wood, W+WWD: Wattle and daub).....6

Figure 2.2 Economic value of the unreinforced masonry and adobe building stock in Central America. 6

Figure 3.1. Retrofitting techniques for URM. Top-left: Ferrocement (Ashraf et al., 2012); top-right: FRP (San Bartolome & Coronel, 2011); bottom-left: PP-bands (Mayorca & Meguro, 2004), bottom-right: Steel-bands (Farooq, 2006). 11

Figure 3.2 Retrofitting techniques for adobe construction. Top left: external steel mesh [CERESIS, 2015]; top right: external synthetic mesh [Varum et al., 2014]; bottom left: steel rebars [Banadaki et al., 2019]; bottom right: timber confinement [Reyes et al., 2019].. 16

Figure 4.1. Non-retrofitted out-of-plane median capacity curves.....23

Figure 4.2 Retrofitted and non-retrofitted median capacity curves. Top-left: MUR+ADO/LWAL+DNO/H:1; top-right: MUR+ADO/LWAL+DNO/H:2; center-left:MUR+CLBRH/LWAL+DNO/H:1; center-right: MUR+CLBRH/LWAL+DNO/H:2; bottom-left: MUR+CBH/LWAL+DNO/H:1, bottom-right: MUR+CBH/LWAL+DNO/H:2. 24

Figure 4.3 Economic value Retrofitted and non-retrofitted in-plane fragility curves for MUR+CBH/LWAL+DNO/H:1 for damage states: slight (top-left), moderate (top-right), extensive (bottom left) and collapse (bottom right). 26

Figure 4.4 Economic Retrofitted and non-retrofitted fragility curves for MUR+CLBRH/LWAL+DNO/H:1 for damage states: slight (top-left), moderate (top-right), extensive (bottom left) and collapse (bottom right).. 27

Figure 4.5 Retrofitted and non-retrofitted fragility curves for MUR+ADO/LWAL+DNO/H:1 for damage states: slight (top-left), moderate (top-right), extensive (bottom left) and collapse (bottom right). 28

Figure 4.6 Retrofitted and non-retrofitted vulnerability curves for MUR/LWAL+DNO/H:1 (top-left), MUR/LWAL+DNO/H:2 (top-right), MUR+ADO/LWAL+DNO/H:1 (bottom-left) MUR+ADO/LWAL+DNO/H:2 (bottom-right).....30

Figure 5.1. Average annual loss (AAL) in USD for the non-retrofitted and retrofitted cases ... 34

Figure 5.2 Highest Benefit Cost Ratio (BCR) at sub-national level in Central America for 1-storey unreinforced masonry, considering only direct losses [left], and considering the total losses [right]. ... 36

Figure 5.3 Highest Benefit Cost Ratio (BCR) at sub-national level in Central America for 2-storey unreinforced masonry, considering only direct losses [left], and considering the total losses [right]. ... 36

Figure 5.4 Highest Benefit Cost Ratio (BCR) at sub-national level in Central America for 1-storey adobe, considering only direct losses [left], and considering the total losses [right]. ... 37

Figure 5.5 Highest Benefit Cost Ratio (BCR) at sub-national level in Central America for 2-storey adobe, considering only direct losses [left], and considering the total losses [right]. ... 37

Figure 5.6 Optimal retrofitting technique (technique with highest BCR ratio when BCR>1) for the 1-storey URM (left) and the 2-storey URM (right) residential building stock. ... 38

Figure 5.7 Optimal retrofitting technique (technique with highest BCR ratio when BCR>1) for the 1- storey adobe (left) and 2-storey adobe (right) residential building stock. ... 38

LIST OF TABLES

Table 2.1. Average dimensions of outer walls for the studied building types in the Central America 7

Table 3.1. Structural performance of different retrofitting techniques for URM. 10

Table 3.2. Cost of retrofitting techniques for URM in Central America and other reference costs [2021 USD/m2 wall].....10

Table 3.3.Structural performance of Adobe under different retrofitting techniques. 15

Table 3.4.Cost of retrofitting techniques for Adobe in Central America and other reference costs [2021 USD/m2 wall].....15

Table 4.1. Structural parameters for the median capacity curves. 23

Table 4.2. Median (θ) and logarithmic standard deviation (β) of the fragility functions defined for each case.....25

Table 4.3. Damage thresholds.....26

Table 4.4.Parameters used for the conversion of the fragility functions into vulnerability functions for economic losses, injured and fatalities. 29

Table 4.5. Average hospitalization time (in days) and average daily cost of injured in infirmaries or intensive care units (in USD).....31

Table 5.1. BCR for the whole country considering only direct (structural) losses 35

Table 5.2. BCR for the whole country considering direct and indirect (fatalities and injuries) losses. 35

LIST OF SYMBOLS

AAL	= Average Annual Loss
BCR	= Benefit Cost Ratio
C	= Cost of retrofitting
e	= Euler's mathematical constant
H	= Storey height
N	= Number of storeys of the structure
r	= Discount Rate
Sa_y	= Yield spectral acceleration
Sa_u	= Ultimate spectral acceleration
Sd_y	= Yield spectral displacement
Sd_u	= Ultimate spectral displacement
t	= Time horizon
Ty	= Fundamental period of vibration
θy	= Yield drift
θu	= Ultimate drift
Γ	= Modal participation factor of the 1st mode
π	= Pi

1. INTRODUCTION

Earthquakes around the world continue to demonstrate the persistent vulnerability of societies to seismic hazards. Although governments, academic institutions, and international organizations have increasingly promoted risk-reduction measures—such as enforcing building codes, encouraging safer construction practices, and developing seismic zonation plans—recent events (e.g., 2016 M7.8 Muisne; 2018 M7.4 Sulawesi; 2020 M5.2 Zagreb; the 2023 M7.8 and M7.5 Kahramanmaras doublet; and the 2026 M7.5 and M7.2 Yumare earthquakes) reveal that substantial gaps remain. A central challenge is that most mitigation strategies prioritize new construction, while older and informal buildings—frequently responsible for most of the damage and casualties—receive comparatively little attention.

As highlighted by Kappos and Dimitrakopoulos [2008], public policy decisions aimed at improving the seismic safety of existing building stock are among the most difficult to implement. Their benefits often materialize only in the long term, and if no damaging earthquake occurs within the lifetime of a retrofitted structure, the value of the intervention may never be perceived. Additionally, some retrofitting techniques appear too expensive when only direct costs are considered [e.g., Liel et al., 2013], but incorporating indirect losses—such as business interruption or medical treatment for injuries—and all its uncertainties, is often challenging.

Among the strategies to quantify the economic feasibility of the interventions, benefit–cost analysis has gained popularity as a tool to support decision makers in evaluating seismic risk-mitigation strategies. An intervention is considered economically viable when its expected benefits exceed its costs (i.e., when the benefit–cost ratio, BCR, is greater than 1). For retrofitting and rehabilitation programs, this methodology is appropriate when benefits can be estimated reliably through a robust seismic risk assessment, uncertainties are properly quantified and propagated, and retrofitting costs are determined in a transparent and context-specific manner. As noted by FEMA [1992], benefit–cost analysis can provide "useful guidance about prospective seismic rehabilitation," although results must be interpreted with caution, acknowledging model assumptions, methodological limitations, and the sensitivity of outcomes to variations in input parameters.

Several studies have applied benefit–cost analysis to evaluate the feasibility of retrofitting, particularly for reinforced concrete structures. Kappos and Dimitrakopoulos [2008] examined optimal strengthening levels for a heterogeneous pre-code reinforced concrete building stock in Thessaloniki. Smyth et al. [2004] assessed the direct benefits and costs of alternative retrofitting measures for a prototype reinforced concrete apartment building in Istanbul. Liel et al. [2013] evaluated three retrofitting strategies for older non-ductile concrete frame buildings in California, incorporating both direct and indirect losses. Additional contributions include Pomonis and Gaspari [2014], who analyzed retrofitting options for reinforced concrete and unreinforced stone masonry buildings in Pylos, Greece, and Valcárcel et al. [2014], who studied the feasibility and prioritization of school retrofitting programs in Latin America.

Among these works, the study by Liel et al. [2013] stands out for its detailed and comprehensive approach, employing nonlinear structural analysis and performance-based earthquake engineering methods for seismic loss estimation. Their findings illustrate how excluding non-structural and indirect losses can make retrofitting appear economically unattractive, particularly for reinforced concrete buildings with high intervention costs. They also show that results are highly sensitive to assumptions regarding retrofitting costs, the performance level achieved, and the selected time horizon for the analysis.

A recurring limitation in many of these efforts is the oversimplification of assumptions regarding retrofitting performance and cost. Several studies rely on hypothetical structural enhancements without specifying the actual interventions required or their realistic implementation costs. For instance, Kappos and Dimitrakopoulos [2008] assumed that applying a generic retrofitting method would reduce the vulnerability of a "low-code" building to match that of a "high-code" building. Similarly, Valcárcel et al. [2014] assumed that adobe and unreinforced masonry buildings could be upgraded to the performance level of reinforced masonry, without detailing the specific interventions or their true costs. Such simplifications limit the applicability of the results, particularly when retrofitting strategies vary widely in cost, feasibility, and expected performance.

FEMA [1992] emphasized that benefit–cost analyses for seismic rehabilitation could be significantly improved by acquiring better data on retrofitting techniques, costs, and the seismic performance of retrofitted structures, as well as more accurate estimates of expected damages and losses. Kappos and Dimitrakopoulos [2008] similarly noted the scarcity of data on the effects of structural mitigation on damage reduction and Smyth et al. [2004] mentions there remains a clear need for more realistic and systematic benefit–cost analyses to support effective earthquake-damage mitigation.

Studies in the last decade have applied benefit–cost analysis to different building types and different structural systems. Jaimes and Niño [2017] examined the prioritization of retrofitting interventions for schools in Mexico City, Carofilis et al. [2020] studied the reduced structural and nonstructural damage, repair costs, time, and injury and death rates for reinforced concrete, precast concrete, and URM school buildings in Italy and Khursheed et al. [2024] evaluated carbon wrapping and concrete jacketing as seismic retrofitting techniques for reinforced concrete hospital buildings.

From the perspective of structural systems, for reinforced concrete buildings, Pomonis and Gaspari [2013], Vitiello et al. [2017], Cardone et al. [2019], and Dumaru et al. [2019] evaluated the economic feasibility of several strengthening strategies. For masonry, Giordano et al. [2018] and Giordano et al. [2020] assessed two common retrofitting techniques for unreinforced stone masonry in Nepal, including the option of incremental intervention and Maio et al. [2020] studied the analysis of intervention techniques for renovation of stone masonry.

More recently, however, the scope of these analyses has expanded beyond the evaluation of seismic risk reduction alone. Villalba et al. [2025] included the cost and improvement in energy performance of retrofitting techniques for reinforced concrete buildings, while Aljawhari et al. [2025] adopted a broader life-cycle perspective that integrates economic, environmental, and functionality-related considerations in the assessment of alternative retrofit strategies for an existing RC structure.

Based on the previous points, this study aims to: 1) present a literature review on economic, practical and applicable retrofitting measures for some of the most vulnerable building classes, 2) provide a database with the cost of retrofitting with different techniques for the countries in Central America, 3) propose a methodology to measure the enhancement and upgrading of the structural performance with the different chosen techniques for an heterogeneous portfolio of buildings that can be easily replicated to other contexts, 4) execute a seismic risk analysis to calculate the losses for the non-retrofitted and retrofitted cases, and finally 5) perform a benefit/cost analysis to establish the feasibility of various strategies for disaster risk reduction in the Central American region.

The present document is organized as follows: in Chapter 2, a characterization of the Central American region and its physical exposure (the residential building stock) is presented. A survey of literature on possible retrofitting techniques and their structural performance enhancements is reported in Chapter 3. The methodology followed to derive fragility curves for both the non-retrofitted and retrofitted structures is described in Chapter 4 and the results of the seismic risk analysis, and the benefit/cost are presented in Chapter 5. Finally, Chapter 6 includes some final remarks on the on-going and future work and some suggestions on possible improvements to the presented methodology.

2. CHARACTERIZATION OF RESIDENTIAL BUILDING STOCK IN THE REGION

For the characterization of the building stock in Central America the exposure model developed by Calderon et al., [2021] for Central America was used. This model covers the residential, commercial, and industrial building stock of the seven Central American countries (i.e., Belize, Costa Rica, Guatemala, Honduras, Nicaragua, Panama, and El Salvador). The model includes the number of buildings at the smallest administrative level, the replacement cost, number of occupants (for residential buildings) and the vulnerability classification according to the GEM Taxonomy [Silva et al, 2022]. In this study, only residential buildings and an occupancy rate of 60% to account for the variation in the occupancy during different times of the day were considered.

According to this exposure model, masonry is the most common type of construction in the region, representing more than 52% of the building stock, and housing approximately 28.4 million people. The distribution of the main types of construction in Central America is depicted in Fig. 1. Additionally, the aggregated economic value (in USD) of the unreinforced masonry and adobe building stock, at the smallest available administrative level, is illustrated in Fig. 2.

Regarding the unreinforced masonry and adobe classes, they represent 36% of the building stock in Central America, housing approximately 15.6 million people. As it can be seen in Fig. 1, unreinforced masonry is the most common typology in Belize (with 38%) and El Salvador (with 27%) and represents around 20% of the building stock in Guatemala, Honduras, Nicaragua, and Panama. With respect to adobe, the distribution of this building typology varies greatly amongst the countries, from being non-existent in Belize to representing 33% of the building stock in Honduras. In Guatemala and El Salvador, this type of construction represents more than 15% of the building stock. Moreover, these types of construction are practically inexistant in Costa Rica due to the strict regulations imposed due to the heavy damage observed in the 1910 ~M6.7 Cartago earthquake [Calderon et al., 2021].

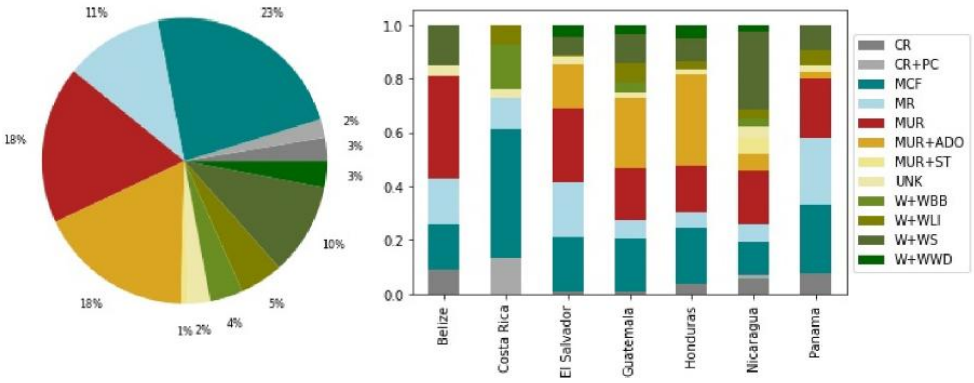


Figure 2.1. Distribution of the number of buildings in Central America (CR: Reinforced concrete, CR+PC: Precast concrete, MCF: Confined masonry, MR: Reinforced masonry, MUR: Unreinforced masonry, MUR+ADO: Adobe, MUR+ST: Stone masonry, UNK: Unknown, W+WBB: Bamboo wood, W'+WLI: Light wood, W+WS: Strong wood, W+WWD: Wattle and daub).

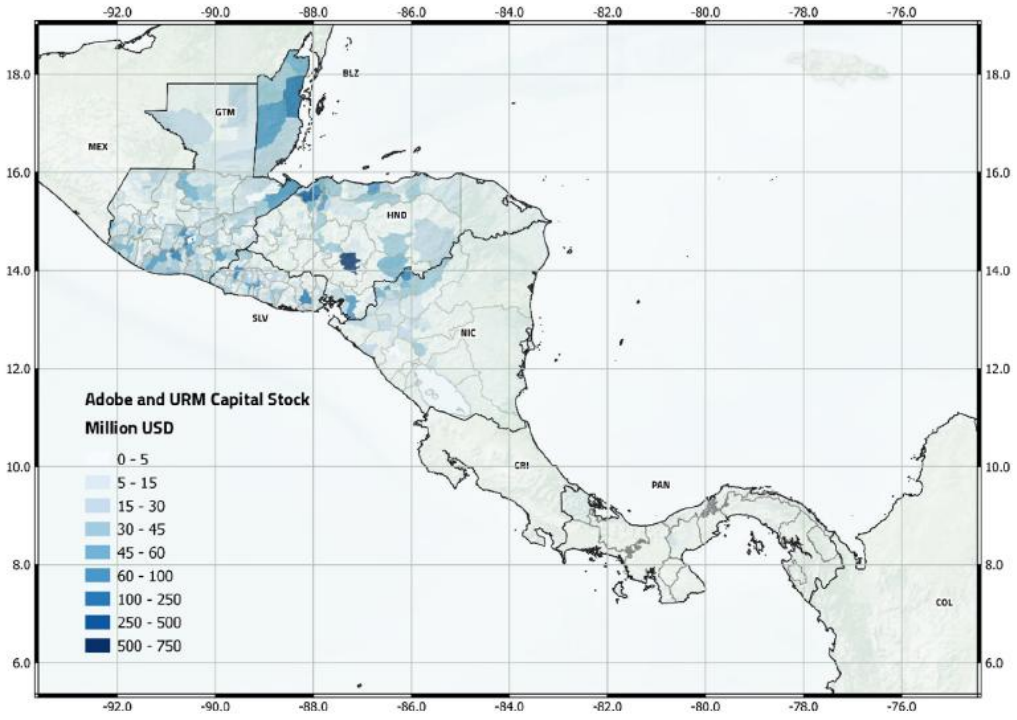


Figure 2.2 Economic value of the unreinforced masonry and adobe building stock in Central America.

It is important to note that within the region there are differences in the type of masonry that is used, with concrete blocks being common in Guatemala, Costa Rica and Panama, while both fire-clay bricks and concrete blocks are used in the other countries. For these latter countries, the concrete block represents a great percentage of new construction, while fire-clay bricks can still be found in older houses. The average dimension of an unreinforced masonry wall and an adobe wall within the region are shown in Table 2.1.

Table 2.1. Average dimensions of outer walls for the studied building types in the Central America

Building Type	Taxonomy	Height [m]	Width[m]
Concrete Block	MUR+CBH	2.8	0.20
Fire Clay Block	MUR+CLBRH	2.8	0.15
Adobe	MUR+ADO	2.6	0.40

3. SELECTION OF RETROFITTING TECHNIQUES

As noted by Costa et al. [2010], a structural system can be improved to better resist seismic actions by enhancing its strength (i.e., increasing its base-shear capacity), its stiffness (potentially reducing displacement demands), or its ductility (i.e., increasing its ability to undergo larger deformations without collapsing). A retrofitting intervention may therefore target one or a combination of these properties to improve overall seismic performance.

The following sections present a review of practical retrofitting techniques applicable to unreinforced masonry and adobe building classes. The focus is placed on interventions that have already been implemented or studied in Central America, as well as those used elsewhere in Latin America that could be realistically adopted in the region. For each technique, its cost and expected structural enhancements are reported. Although additional retrofitting strategies exist for these construction types, this study concentrates on interventions that—based on previous projects and documented applications, are considered feasible in terms of cost, required technology, and regional construction practices.

3.1 RETROFITTING TECHNIQUES FOR UNREINFORCED MASONRY BUILDINGS

Non-engineered masonry construction or unreinforced masonry (URM) accounts for 18% of the residential building stock in Central America according to Calderon et al. [2021]; and it represents one of the most vulnerable building classes [e.g., Martins et al, 2021]. According to Daniell [2014]; 57% of worldwide earthquake fatalities from 1900 to 2012 were caused by the collapse of masonry buildings. The high vulnerability is due to a wide range of factors including the structure's brittle behaviour, large mass, low ductility, low tensile strength, and weak connections between all structural elements.

Many retrofitting techniques have been proposed worldwide to enhance the seismic performance of URM buildings, focusing particularly on the improvement of the member connections. Such interventions aim at avoiding the out-of-plane local failures that lead to many of the casualties and injuries in seismic events. These include the use of fibre reinforced polymers (FRP), ferrocement and shotcrete overlay, confinement with RC

elements, addition of steel and polymer bands or steel cables, application of synthetic meshes and post-tensioning, amongst others Ashraf et al. [2012]. As stated by Nayak and

Table 3.2. Structural performance of different retrofitting techniques for URM.

Technique	Stiffness	Lateral Strength	Ductility	Cost*	References	Country
Ferrocement	1.52	1.07	-	12.1%	Abrams et al. [2007]	USA
	1.68	2.1	1.15		Ashraf et al. [2012]	Pakistan
	2.45	2.06	0.8		Ahmad et al. [2015]	Pakistan
	1.90	1.1-1.5	0.8-1.2		Shabdin et al. [2019]	Iran
	2.00	2.6	1.1		Lopez et al. [2013]	Colombia
	1.55	2.2-2.3	-		Sandoval et al. [2021]	Colombia
	1.7	**2.1**	**1.0**			
FRP	1.0	1.15-1.65	1.0-1.2	14.3%	Marcari et al. [2007]	Italy
	1.0	1.5-1.8	1.15		Alcaino & Sta Maria [2008]	Chile
	0.5	1.2	1.2		San Bartolome et al. [2011]	Peru
	0.8-1.0	1.3-1.5	0.9-1.0		Ramirez & Carreon [2004]	Mexico
	1.0	1.27-1.55	1.1		Arias and Lopez [2018]	Costa Rica
	1.0	**1.2-1.8**	**1.1**			
PP-Band	1.0	1.29-1.65	-	10.4%	Nayak & Dutta [2016]	India
	0.8-1.0	1.1-1.5	1.0		Ramirez & Carreon [2004]	Mexico
	1.0	0.87-1.0	1.0-1.2		Mayorca & Meguro [2004]	Japan
	1.0	1.0-1.65	1.0-1.5		Banerjee et al. [2019]	India
	1.0	**1.0-1.65**	**1.1**			
Steel Bands	1.0	1.3-1.9	1.0	10.1%	Farooq et al. [2006]	Pakistan
	0.8	1.6-1.9	1.0		Ramirez & Carreon [2004]	Mexico
	1.0	1.6-2.0	-		Farooq et al. [2014]	Pakistan
	1.0	**1.3-1.9**	**1.0**			

* As percentage of replacement cost

Table 3.3. Cost of retrofitting techniques for URM in Central America and other reference costs [2021 USD/m2 wall].

Country	Ferrocement	FRP	PP Band	Steel Bands
Belize	38	45	32	31
Costa Rica	-	-	-	-
El Salvador	21	25	18	18
Guatemala	24	28	21	20
Honduras	20	24	17	17
Nicaragua	24	28	21	20
Panama	30	35	25	25

Colombia	31	37	26	26
Australia	35	50-70	7% cost house	-

Dutta [2016], URM retrofitting methods in developing countries should be able to withstand the demand (in terms of strength and displacement) and improve the integrity of the structures by ensuring appropriate interlocking of orthogonal walls, while being economically and practically feasible.

A brief description of the selected retrofitting techniques is presented in the following subsections, while the changes caused by each intervention in terms of strength, stiffness, and ductility (for the in-plane failure mechanism) are presented in Table 3.1 and some examples are shown in Figure 3.1. These changes are represented by the ratio between the original and modified structural parameter and have been collected from the literature based mostly on experimental campaigns. Given the differences in the characteristics of the existing studies, different ratios have been found in the literature for each retrofitting technique. A list with all the proposed ratios found in the literature is shown, and then the median values assumed for the study are indicated. Additionally, for each technique, studies on the out-of-plane failure prevention mechanism are presented.



Figure 3.3. Retrofitting techniques for URM. Top-left: Ferrocement (Ashraf et al., 2012); top-right: FRP (San Bartolome & Coronel, 2011); bottom-left: PP-bands (Mayorca & Meguro, 2004), bottom-right: Steel-bands (Farooq, 2006).

The costs (including labor force) for each retrofitting technique are based on unitary costs reported in studies by Ahumada Forero [2015]; Daniell & Schafer [2014]; Smith and Redman [2009]; Ramírez de Alba & Carreon [2004] and Build Change & AGIES [2019]. Ahumada Forero report specific costs for each retrofitting technique of URM for the case of Colombia, including plaster or ring beams if required. For each technique, the costs were calculated considering a 75–80 m2 house (as assumed for these building types in Calderon et al. [2021]; and as reported in Build Change & AGIES [2019]. In this way, considering the perimeter and the height of the structures, it was possible to calculate the cost per retrofitted square meter of wall. Later, the unitary costs were adjusted for each country (using local labour and material costs), and the total cost of each intervention was estimated based on the size and wall area of each building class. The ratios of the retrofitting intervention costs to the total replacement cost are presented in Table 3.1, while in Table 3.2 the costs per square meter of retrofitted wall per country are provided.

3.1.1 Surface Treatment – Ferrocement

Ferrocement, which consists of a steel welded wire mesh connected with screws to the masonry surface and later covered with 2 or 3 cm of plaster (see Fig. 3.1), is a popular URM retrofitting technique in developing countries, given the easiness of its application, low cost, and fast application [Ashraf et al., 2012 and Ahmad et al., 2015]. This material should be connected to the foundation and a ring beam to avoid local (out-of-plane) failure mechanisms. According to Ashraf et al. [2012], URM walls retrofitted with this technique experienced a significant increase in stiffness and strength (68 and 110%, respectively). Their analyses also reported other important benefits including a delay in the appearance of cracks and the occurrence of more ductile failure mechanisms.

Similar results were obtained by Ahmad et al. [2015] for tests conducted at the University of Engineering and Technology in Peshawar, Pakistan. These authors reported a strength and stiffness increase of 106% and 145% for the retrofitted structure, respectively. Among other studies, Abrams et al. [2007] retrofitted masonry piers, and reported an increase in stiffness of 52%. In Latin America, Lopez et al. [2013] and Sandoval et al. [2021] reported enhancements in strength and stiffness of 200% and 250% and 150% and 180%, respectively, for fired brick unreinforced masonry walls. This intervention was also used to retrofit schools in Nepal [Anwar et al., 2016] and has been used in Central America by international organizations such as Build Change for the retrofitting of unreinforced masonry in Guatemala [Build Change & AGIES, 2019], while it is included in building codes from other Latin American countries such as Colombia. Considering the out-of-plane behaviour, studies including Kadam et al. [2015] in India and Baena [2019] in Colombia, have demonstrated that the ferrocement reinforcement provides a connection between perpendicular walls that increases the out-of-plane resistance of the wall up to four times, and in this way prevents the local brittle failures in this direction.

3.1.2 External fibre reinforced polymers (FRP)

Retrofitting with externally applied fibre-reinforced polymer (FRP) meshes (see Fig. 3.1) has been the subject of several studies worldwide. This intervention presents several advantages over other techniques (e.g., shotcreting or the inclusion of structural frames), as FRPs are lighter and stronger, less invasive and disruptive, and easier to install [Mahmood and Ingham, 2011].

Marcari et al. [2007] performed diagonal compression tests on walls retrofitted with both GFRP (glass) and CFRP (carbon). Compared with the non-retrofitted cases, the strengthened specimens achieved strengths 20% to 70% higher, while only negligible differences were observed in stiffness and ductility. Similarly, Alcaíno and Santa María [2008] performed cyclic shear tests on walls retrofitted with GFRPs and CFRPs arranged in different diagonal and horizontal configurations. Their results showed strength increases between 50% and 80%, with no significant changes in stiffness or ductility.

Within the region, experimental campaigns have also been conducted in Costa Rica [Arias and López, 2018], reporting increases of 27% to 55% in strength and about 10% in ductility. Regarding out-of-plane failure, Hoeppner et al. [2002] and Tan and Patoary [2004] showed that this mechanism can be prevented if adequate FRP anchorage is ensured, highlighting the importance of trained workmanship. Nevertheless, this intervention is relatively passive and, despite the reported increase in strength, may not prevent low levels of damage.

3.1.3 Polymer and steel bands

Polymer bands placed around external walls, arranged in a mesh pattern and connected through holes at the intersection points before being plastered, have been investigated by several authors. Nayak and Dutta [2016] reported increases in strength capacity ranging from 29% to 65% for specimens retrofitted with PP-bands (polypropylene bands). Similarly, Banerjee et al. [2019] reported strength ratios between 1.0 and 1.65 and ductility ratios between 1.0 and 1.5. Regarding PP-bands, Mayorca and Meguro [2004] concluded that, although they did not significantly increase the lateral strength capacity of walls, they substantially improved ductility, with retrofitted specimens displaying approximately twice the ductility of their non-retrofitted counterparts (see Fig. 3.1).

On the same topic, Ramírez de Alba and Carreón Guardado [2004] studied the behaviour of URM walls retrofitted with steel and plastic straps using multiple configurations. Although the retrofitted and non-retrofitted specimens exhibited similar stiffness, walls strengthened with plastic bands showed an increase in strength capacity between 10% and 50%, while those retrofitted with steel bands achieved increases between 60% and 90%. In both cases, ductility increased by approximately 20%. Farooq et al. [2006] also investigated the effectiveness of steel-strip retrofitting through a series of compression and shear tests

on walls wrapped with steel strips in different configurations (see Fig. 3). Their results indicated increases in strength capacity ranging from 30% to 90%.

Regarding the out-of-plane performance, according to the comprehensive literature review by Sathiparan [2020], all reported PP-band retrofitted models subjected to shaking table tests withstood accelerations of up to 0.6 g with only moderate damage and without exhibiting local out-of-plane failure.

3.2 RETROFITTING TECHNIQUES FOR ADOBE BUILDINGS

Adobe and mud walls remain common construction types in several Central American countries, accounting for more than 12% of the residential building stock according to Calderón et al. [2021]. Their widespread use is largely driven by the availability of construction materials, low construction costs, and the possibility of building without skilled labour. However, these structures are known to be highly vulnerable to seismic shaking due to their large mass, susceptibility to significant inertial forces, low tensile strength, and brittle behaviour [Varum et al., 2014; Dowling, 2004]. Consequently, they have been responsible for substantial economic losses and casualties in past earthquakes (e.g., the 1972 M6.2 Managua, 1976 M7.5 Guatemala, 1986 M5.6 El Salvador, 2001 M7.7 El Salvador, 2003 M6.6 Bam, 2007 M8.8 Pisco, and 2015 M7.8 Gorkha earthquakes). In the 2001 M7.7 El Salvador earthquake, adobe buildings accounted for 57% of affected houses, 68% of destroyed houses, and 40% of damaged houses [Dowling, 2004].

Among the possible collapse mechanisms for this type of construction, wall overturning is reported as the most common and devastating due to out-of-plane actions. This failure mechanism is primarily associated with inadequate connections to perpendicular walls, a limited number of cross walls, and the absence of binding elements such as tie beams or tie rods [Illampas et al., 2013]. Other common damage patterns include diagonal in-plane cracking, cracking near openings, vertical cracking at wall intersections, disintegration of the upper portions of walls, collapse of gable wall tops, and separation between roofs and supporting walls [Dowling, 2004; Vargas-Neumann et al., 2018].

Significant efforts have been devoted to developing retrofitting techniques that address these structural deficiencies. As noted by Vargas-Neumann et al. [2018], the key objective when retrofitting adobe houses is to ensure adequate connections between structural elements while providing sufficient deformation capacity to prevent collapse. The retrofitting techniques described in the following subsections contribute to both in-plane and out-of-plane collapse prevention. As previously presented for URM buildings, a brief description of each technique is provided, while the corresponding changes in strength, ductility, and stiffness are summarised in Table 4. The total costs for each country are reported in Table 3.3.

Table 3.4. Structural performance of Adobe under different retrofitting techniques.

Technique	Stiffness	Lateral Strength	Ductility	Cost*	References	Country
External mesh (1 storey) or Steel mesh (2	1.1	2.3	1.8	12.1%	Herrera et al. [2008]	Mexico
	-	1.45-2.0	1.5		Yamin et al. [2007]	Colombia
	1.0	1.7-2.5	2.0-2.5		Reyes et al. [2019]	Colombia
	1.0	2.0	**2.0**			
FRP	1.0	1.0	1.1	11.1%	Reyes et al. [2019]	Colombia
	1.0	1.25	1.8		Oliveira et al. [2010]	Portugal
	-	1.0-1.4	1.8		Torrealva et al. [2012]	Peru
	1.0	1.23	3.0		Figuereido et al. [2013]	Portugal
	-	1.2	2.0		Varum et al. [2014]	Portugal
	1.0	**1.2**	**1.8**			
PP-Band	1.0	1.7-2.4	1.1	12.8%	Banaki et al. [2019]	Iran
	1.0	**2.1**	**1.1**			
Steel Bands	1.2	1.7	1.7	10.0%	Farooq et al. [2006]	Pakistan
	1.4	2.0	4.0		Ramirez & Carreon [2004]	Mexico
	1.0	1.7	3.3		Reyes et al. [2019]	Pakistan
	1.2	**1.7**	**3.0**			

* As percentage of replacement cost

Table 3.5. Cost of retrofitting techniques for Adobe in Central America and other reference costs [2021 USD/m2 wall].

Country	Steel Mesh	Synthetic Mesh	Steel Bars	Timber Conf.
Belize/Costa Rica	-	-	-	-
El Salvador	21	20	23	18
Guatemala	24	22	25	20
Honduras	20	18	21	17
Nicaragua	24	22	25	20
Panama	30	27	31	25
Colombia	31	28	33	25
Australia	35	45	-	-



Figure 3.4 Retrofitting techniques for adobe construction. Top left: external steel mesh [CERESIS, 2015]; top right: external synthetic mesh [Varum et al., 2014]; bottom left: steel rebars [Banadaki et al., 2019]; bottom right: timber confinement [Reyes et al., 2019]..

3.2.1 External Steel Mesh

The first external mesh system used and tested for adobe structures consisted of welded steel meshes with vertical and horizontal strips covered by a sand-cement render, applied on both sides of the wall and connected through wires passing across the wall thickness (see Fig. 3.2). This system was shown to increase wall strength, control displacements, and delay collapse [Dowling, 2006]. It also demonstrated satisfactory performance during the 2001 M8.4 Arequipa and 2007 M8.0 Pisco earthquakes in Peru in buildings that had previously been retrofitted using this technique [San Bartolome et al., 2008].

Yamín et al. [2007] conducted an experimental campaign on adobe walls retrofitted with external steel meshes and observed increases of 45% to 100% in strength capacity and about 50% in ductility. In a similar study, Herrera et al. [2008] reported increases of nearly 100% in both strength and ductility. Reyes et al. [2019] subsequently performed cyclic tests

on steel mesh-reinforced adobe walls, finding increases in strength and displacement capacity ranging from 10% to 150%. Within the region, this technique has also been applied in the retrofitting of buildings located in historic centres [JICA, 2010; FUNDASAL, 2014]. Regarding out-of-plane behaviour, as in the ferrocement case, the intervention can prevent out-of-plane failure mechanisms provided that adequate connections between all structural elements are ensured.

3.2.2 External Synthetic Mesh

Synthetic mesh retrofitting emerged from efforts to replicate the benefits of mesh wrapping in adobe walls using locally available and low-cost materials. Various systems based on geogrids (i.e., polymeric materials formed by intersecting ribs with regular apertures), polymer-based composites, and other plastic compounds have been proposed for strengthening adobe structures [Varum et al., 2014]. Compared with unreinforced adobe walls, geogrid-retrofitted specimens exhibited similar initial stiffness while achieving increases in strength capacity of approximately 25% to 40% and nearly double the ductility [Oliveira et al., 2010; Torrealva et al., 2008]. With respect to out-of-plane behaviour, shaking table tests conducted by Sathiparan [2020] and Torrealva [2012] showed that retrofitted structures were able to withstand acceleration levels of 0.7 g and 0.8 g, respectively, without developing out-of-plane failure mechanisms.

3.2.3 External near-surface mounted (NSM) steel rebars

The external NSM (near-surface-mounted) steel rebar technique consists of installing horizontal and vertical reinforcing bars within grooves cut into both faces of the wall. Banadaki et al. [2019] reported increases of 70% to 140% in lateral strength and 50% to 150% in ductility for specimens retrofitted using this method. The authors also highlighted several advantages over plaster-based retrofit techniques, including greater resistance to debonding and reduced aesthetic impact. To the authors' knowledge, this is the only intervention that has not yet been applied within the region; therefore, the workmanship requirements were defined based on those adopted for the other retrofit techniques.

3.2.4 Timber confinement

Timber confinement consists of installing timber elements to increase flexural strength and improve the integrity of the structural system, enabling the building to behave as a composite earth-and-wood structure [Yamín et al., 2007]. The timber elements provide confinement, thereby reducing the likelihood of failure [Ruiz et al., 2014]. This technique is particularly attractive due to its ease of application, limited invasiveness, and low material cost [Yamín et al., 2004]. Experimental testing on both full-scale and reduced-scale walls conducted by Yamín et al. [2003] demonstrated significant improvements in deformation and energy dissipation capacity. The technique increased strength capacity by approximately 100% and ductility by nearly 400% [Yamín et al., 2007]. More recently, Reyes

et al. [2019] confirmed these findings, reporting increases of about 70% in strength capacity and ductility improvements of up to five times those of non-retrofitted walls. Within the region, cane confinement was also investigated through the TAISHIN project [FUNDASAL, 2014]. As a confinement-based intervention, it is expected to effectively prevent out-of-plane failure mechanisms.

4. VULNERABILITY ASSESSMENT OF RETROFFITED CASES

To evaluate the potential impact of each retrofitting technique through benefit-cost analysis, it is essential to quantify the vulnerability associated with each intervention and the uncertainty of following the specific methodology for its derivation. For this purpose, the Vulnerability Modeller's Toolkit (VMTK) developed by Martins et al. [2021] was employed. The VMTK is an open-source platform for deriving fragility and vulnerability functions. It employs nonlinear time-history analyses (NLTHA) to estimate the structural response of single-degree-of-freedom (SDOF) oscillators subjected to a suite of ground-motion records, and then applies cloud analysis [Jalayer et al., 2015] to relate ground-motion intensity measures (IMs) to an engineering demand parameter (EDP). The structural and dynamic properties of each SDOF oscillator are defined through one or more capacity curves, assumed to represent the seismic behaviour of the corresponding building class. The resulting IM-EDP relationship can be combined with a damage criterion (i.e., a model defining EDP thresholds for each damage state) to derive fragility functions (i.e., the probability of exceeding specific damage states conditional on an IM), as described in Section 4.2. In turn, each fragility model can be converted into a vulnerability model (i.e., the probabilistic distribution of loss ratios conditional on an IM) through a damage-to-loss model (i.e., a model defining the probability distribution of loss ratios for each damage state), as described in Section 4.3. Further details regarding the calculation workflow can be found in Martins et al. [2021].

One of the major advantages of using this tool is that it can propagate the uncertainty in each of the parameters obtained throughout the procedure. As part of the RESURBAN project, which addressed the resilience of buildings in urban areas across the European Union, Maio and Tsionis [2016] reviewed and evaluated analytical fragility/vulnerability curves and identified the main sources of uncertainty involved in their derivation. The report highlighted five major sources of uncertainty: (1) mathematical modelling uncertainty, which depends on both the level of detail of the selected model and the adopted performance criteria; (2) uncertainty in structural characteristics, including geometric configuration, mechanical properties, and structural details; (3) uncertainty in the representation of seismic demand, which should capture record-to-record variability, site effects, and other source-related characteristics; (4) uncertainty in damage-threshold modelling, particularly in the definition of global limit states; and (5) uncertainty associated

with fragility-curve fitting, which depends on the specific fitting procedure adopted [Maio and Tsionis, 2016]. For a fragility model to be robust and consistent, all these sources of uncertainty should be considered and adequately quantified and propagated. In the following sections, each source of uncertainty is identified and the methodology adopted to account for and propagate it is described.

It is important to note that the use of SDOF oscillators for vulnerability analysis presents some limitations, particularly regarding the explicit representation of horizontal irregularities (e.g., torsional effects) and higher-mode contributions. Nevertheless, this approach has been widely adopted in the literature for the derivation of fragility models used in large-scale seismic risk assessments [Akkar et al., 2005; Erberik, 2007; Suzuki and Iervolino, 2019], including the ones developed in this study. Moreover, it enables straightforward modifications of key structural properties, such as strength, stiffness, and ductility, facilitating the evaluation of different retrofit interventions. Martins and Silva [2021] used the VMTK to derive a set of fragility and vulnerability functions for some of the most common building classes worldwide, including the construction types considered in this study and representative of the region under analysis. All source code and input parameters (Tables 3.1, 3.3, and 4.1) used in this section are publicly available, allowing the results presented herein to be fully reproduced.

4.1 QUANTIFICATION OF UNCERTAINTY IN THE VMTK

When conducting vulnerability and risk analyses of building portfolios, the selection of an appropriate numerical model is critical given the limited availability of both information and computational resources and for the correct **quantification of mathematical modelling uncertainty**. Therefore, a balance must be achieved between accuracy and efficiency. For large building populations, simplified approaches such as nonlinear static procedures or nonlinear time-history analyses of single-degree-of-freedom (SDOF) systems are often preferred over nonlinear dynamic analyses of multi-degree-of-freedom (MDOF) systems. Although these simplifications present important limitations, including the neglect of higher vibration modes and the potential underestimation of uncertainty in the structural response, they have been shown to provide satisfactory results when compared with more detailed dynamic models [Silva et al., 2014]. Nevertheless, the accuracy and reliability of the results remain "highly dependent on the expertise of the operator in choosing the underlying simplifications and assumptions" [Maio and Tsionis, 2016].

To quantify and propagate the **uncertainty in structural characteristics**, while accounting for building-to-building variability, 150 capacity curves were generated for each

building class (retrofitted and non-retrofitted) using a Monte Carlo simulation. The capacity curves derived and described in this section 4.2 were taken as median representations, and the coefficients of variation reported by Silva et al. [2014] and Borzi et al. [2008] were used to generate normally distributed samples around these median curves, considering values within one standard deviation of the median.

Regarding the variability of the structural parameters and the **uncertainty in damage threshold modelling**, Borzi et al. [2008] reported coefficients of variation of 35% for S_{dy} and 30-35% for S_{du} , depending on the percentage of voids in masonry structures. Silva et al. [2014] reported coefficients of variation of 35% for Sau , 24% for S_{dy} , and 41% for S_{du} , based on a sample of 100 randomly generated reinforced concrete frames that accounted for variability in the material and geometric properties of typical Turkish buildings. Similarly, Parisi and Augenti [2012] assessed this source of uncertainty for URM buildings using a typical Southern European residential building as the index structure. Their study reported coefficients of variation ranging from 11% to 55% for ultimate spectral displacement (S_{du}) and from 8% to 24% for spectral acceleration (S_{au}). Among the available studies, the coefficients of variation reported by Silva et al. [2014] were adopted for the adobe building classes, while those proposed by Borzi et al. [2008] were used for the unreinforced masonry classes, assuming no correlation between the spectral displacement and spectral acceleration parameters.

To consider the **uncertainty in the hazard parameters**, the VMTK has different options, however the one used was the one that includes all records provided by the user. In this case the ones obtained for Central America in the CCARA project were considered as the idea was to make a country-wide analysis. For similar analyses for specific sites, the use of the conditional spectrum method would be more accurate, as it considers detailed disaggregation of the hazard of the specific site. In any case, by being able to model multiple ground motions, the uncertainty on hazard can be computed and propagated.

Finally, for modelling the fragility, and quantifying in some way the **uncertainty in the fragility curve/model fitting**, the lognormal cumulative distribution, extensively used in literature for this purpose, is selected, considering its simplicity compared to other parametric or nonparametric distributions [Porter et al., 2007]. The lognormal parameters (logarithmic mean, logarithmic standard deviation and R factor – which reflects the goodness of fit) for each building typology and each damage state are computed from the capacity curves and fragility curves for the retrofitted and non-retrofitted cases are derived. Later, this uncertainty in the lognormal parameters is propagated to the vulnerability curves by assuming mean damage ratios of each damage state.

4.2 DEFINITION OF THE CAPACITY CURVES

4.2.1 In-plane behaviour

As described by Villar-Vega et al. [2017], capacity curves for equivalent in-plane SDOF systems can be defined using the following structural parameters: number of storeys, inter-storey height, elastic (Tel) and yielding (T_y) periods, yielding drift (θ_y), ultimate drift (θ_u), and backbone model type (i.e., bilinear, trilinear, or quadrilinear). For the original configuration of the building classes considered herein (unreinforced masonry and adobe), region-specific input values reported by Villar-Vega et al. [2017], Martins and Silva [2021], and Tables 3.1 and 3.3 were adopted. These values were initially defined through consultation with local experts during workshops conducted within the Caribbean and Central America Risk Assessment (CCARA) project and were subsequently refined based on the results of probabilistic seismic risk analyses for the region [Calderón et al., 2021]. The corresponding vulnerability functions were then derived using the VMTK.

These capacity curves are characterised by a trilinear backbone model, comprising an initial elastic branch, whose slope is defined by the elastic period of vibration, followed by a branch representing the onset of damage and the associated elongation of the vibration period. The model then assumes that the maximum base shear capacity is reached, with collapse occurring at the ultimate global drift. For the retrofitted cases, the original capacity curves were modified according to the strength, stiffness, and ductility factors previously presented (see Tables 3.1 and 3.3). The resulting capacity curves for each building class, also identified according to the GEM taxonomy [Silva et al., 2022], are presented in Table 4.1 and Fig. 4.2, considering both types of unreinforced masonry commonly found in the region: fired-clay brick and concrete block masonry.

4.2.2 Out-of-plane behaviour

For the out-of-plane failure mechanism, wall bending is modelled using the simplified linearised displacement-based procedure proposed by Doherty et al. [2002]. In this approach, the wall is idealised as an SDOF oscillator that moves as a rigid block according to the displacement profile of a rocking wall. Since the walls behave as rigid bodies rotating about pivot points, the capacity curve for the out-of-plane mechanism can be represented using a bilinear force-displacement relationship. However, subsequent experimental studies indicated that the actual response follows a curvilinear profile [Sumerente et al., 2020]. For this reason, a trilinear capacity curve was adopted, with parameters defined based on the equivalent wall width and mass, as proposed by Doherty et al. [2002], together with the wall height and three characteristic displacements (Δ_1, Δ_2, and Δu) reported by Sumerente et al. [2020] that define the end of each branch. The idealised capacity curves for the different building classes are presented in Fig. 4.1, while the corresponding parameters are reported in Table 4.1. Additional details regarding the derivation of these capacity curves can be found in Doherty et al. [2002] and Sumerente et al. [2020].

Table 4.6. Structural parameters for the median capacity curves.

Typology	Retrofit	S_{del} (m)	S_{ael} (g)	S_{dy} (m)	S_{ay} (g)	S_{du} (m)	S_{au} (g)
Concrete Blocks URM with 1 storey	None (in-plane)	0.0005	0.300	0.004	0.600	0.021	0.606
MUR+CBH/LWAL+DNO/H:1	None (out-of-plane)	0.0173	0.0429	0.0533	0.0429	0.1333	0
	Ferrocement	0.0006	0.6299	0.0047	1.2597	0.026	1.2723
	FRP	0.0008	0.4799	0.006	0.9598	0.037	0.9694
	PP-band	0.0006	0.3974	0.005	0.7948	0.0307	0.8027
	Steel band	0.0008	0.4798	0.006	0.9598	0.0337	0.9694
Concrete Blocks URM with 2 storeys	None (in-plane)	0.0009	0.1800	0.008	0.359	0.042	0.363
MUR+CBH/LWAL+DNO/H:2	None (out-of-plane)	0.0173	0.0857	0.0533	0.0857	0.1333	0
	Ferrocement	0.0012	0.3771	0.0093	0.7542	0.0520	0.7618
	FRP	0.0015	0.2873	0.0121	0.5747	0.0741	0.5804
	PP-band	0.0013	0.2380	0.0100	0.4759	0.0614	0.4807
	Steel band	0.0015	0.2873	0.0121	0.5747	0.0674	0.5804
Clay Bricks URM with 1 storey	None (in-plane)	0.0003	0.239	0.003	0.478	0.0160	0.482
MUR+CLBRH/LWAL+DNO/H:1	None (out-of-plane)	0.0152	0.0375	0.0467	0.0375	0.1167	0
	Ferrocement	0.0004	0.5015	0.0034	1.0030	0.0195	1.0130
	FRP	0.0005	0.3821	0.0044	0.7642	0.0277	0.7719
	PP-band	0.0005	0.3164	0.0036	0.6329	0.0230	0.6392
	Steel band	0.0005	0.3821	0.0044	0.7642	0.0252	0.7719
Clay Bricks URM with 2 storeys	None	0.0007	0.143	0.005	0.286	0.032	0.289
MUR+CLBRH/LWAL+DNO/H:2	None (out-of-plane)	0.0152	0.075	0.0467	0.075	0.1167	0
	Ferrocement	0.0008	0.3003	0.0068	0.6006	0.039	0.6066
	FRP	0.0011	0.2288	0.0088	0.4576	0.0556	0.4621
	PP-band	0.0009	0.1895	0.0073	0.3789	0.0460	0.3827
	Steel band	0.0011	0.2288	0.0088	0.4576	0.0505	0.4621
Adobe with 1 storey	None	0.0003	0.191	0.003	0.382	0.013	0.386
MUR+ADO/LWAL+DNO/H:1	None (out-of-plane)	0.0613	0.0885	0.1533	0.0885	0.3067	0
	Steel mesh	0.0006	0.3821	0.0051	0.7643	0.0500	0.7719
	Synthetic mesh	0.0004	0.2293	0.0031	0.4586	0.0270	0.4632
	Steel bars	0.0007	0.4012	0.0053	0.8025	0.0289	0.8105
	Timber confinement	0.0004	0.3248	0.0035	0.6496	0.0517	0.6561
Adobe with 2 storeys	None	0.0006	0.102	0.005	0.205	0.025	0.207
MUR+ADO/LWAL+DNO/H:2	None (out-of-plane)	0.0613	0.1769	0.1533	0.1769	0.3067	0
	Steel mesh	0.0013	0.2048	0.0102	0.4096	0.1000	0.4137
	Synthetic mesh	0.0008	0.1229	0.0061	0.2457	0.05405	0.2482
	External steel bars	0.0013	0.215	0.0107	0.43	0.0578	0.4343
	Timber confinement	0.0009	0.1741	0.007	0.3481	0.1034	0.3516

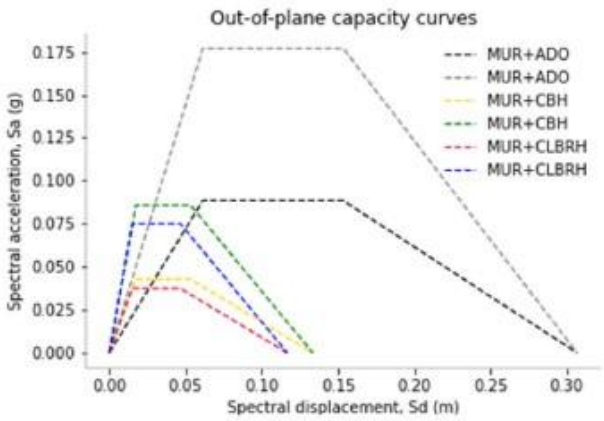


Figure 4.5. Non-retrofitted out-of-plane median capacity curves.

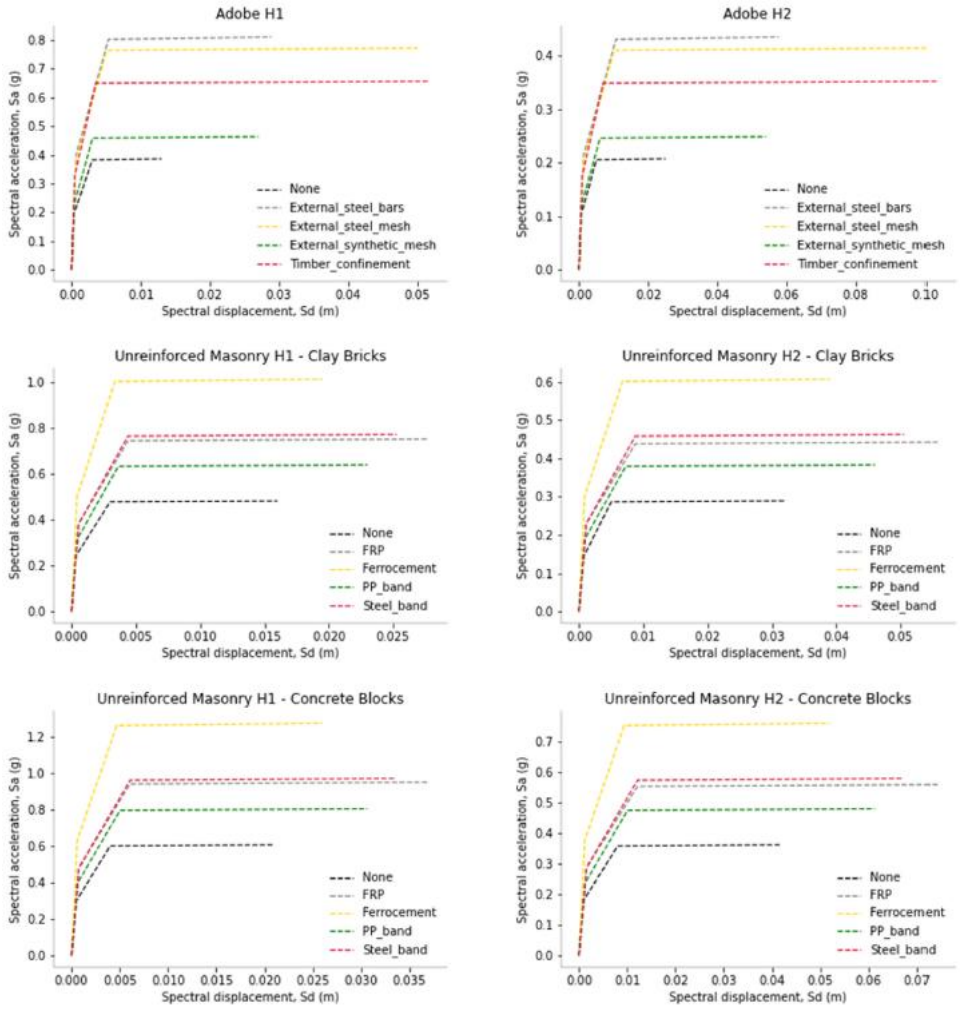


Figure 4.6 Retrofitted and non-retrofitted median capacity curves. Top-left: MUR+ADO/LWAL+DNO/H:1; top-right: MUR+ADO/LWAL+DNO/H:2; center-left:MUR+CLBRH/LWAL+DNO/H:1; center-right: MUR+CLBRH/LWAL+DNO/H:2; bottom-left: MUR+CBH/LWAL+DNO/H:1, bottom-right: MUR+CBH/LWAL+DNO/H:2.

4.3 DERIVATION OF FRAGILITY FUNCTIONS

The fragility functions were derived using a damage criterion defined as a function of the yielding and ultimate displacements of each building class [Martins and Silva, 2021; Villar-Vega et al., 2017]. This approach results in damage thresholds that are specific to each building class and retrofit intervention, rather than relying on fixed drift limits that may not accurately reflect the actual structural capacity. For the in-plane response, four damage states (slight, moderate, extensive, and complete damage) were considered, consistent with damage scales adopted in HAZUS [Federal Emergency Management Agency (FEMA), 2004] and by Martins and Silva [2021]. For the out-of-plane mechanism, only a single damage state was considered, following the approach adopted in similar studies [Borzi et al., 2008].

Table 4.7. Median (θ) and logarithmic standard deviation (β) of the fragility functions defined for each case.

Typology	Retrofit	IM	Slight		Moderate		Extensive		Collapse	
			θ	β	θ	β	θ	β	θ	β
Concrete Blocks URM with 1 storey MUR+CBH/LWAL+DNO/H:1	None (ip)	PGA	0.45	0.56	0.76	0.56	1.01	0.56	1.22	0.56
	None (oop)	PGA	–	–	–	–	–	–	0.21	0.85
	Ferrocement	PGA	1.04	0.45	1.67	0.45	2.15	0.45	2.53	0.45
	FRP	PGA	0.83	0.48	1.46	0.48	1.95	0.48	2.34	0.48
	PP-band	PGA	0.66	0.5	1.17	0.5	1.56	0.5	1.88	0.5
	Steel band	PGA	0.82	0.48	1.39	0.48	1.83	0.48	2.19	0.48
Concrete Blocks URM with 2 storeys MUR+CBH/LWAL+DNO/H:2	None (ip)	Sa(0.3s)	0.53	0.64	1.09	0.64	1.6	0.64	2.07	0.64
	None (oop)	Sa(0.3s)	–	–	–	–	–	–	0.18	0.92
	Ferrocement	Sa(0.3s)	1.04	0.57	2.1	0.57	3.03	0.57	3.86	0.57
	FRP	Sa(0.3s)	0.89	0.6	1.95	0.6	2.91	0.6	3.76	0.6
	PP-band	Sa(0.3s)	0.7	0.64	1.58	0.64	2.38	0.64	3.11	0.64
	Steel band	Sa(0.3s)	0.89	0.59	1.86	0.59	2.74	0.59	3.52	0.59
Clay Bricks URM with 1 storey MUR+CLBRH/LWAL+DNO/H:1	None (ip)	PGA	0.34	0.58	0.57	0.58	0.76	0.58	0.91	0.58
	None (oop)	PGA	–	–	–	–	–	–	0.15	0.99
	Ferrocement	PGA	0.8	0.46	1.31	0.46	1.7	0.46	2.01	0.46
	FRP	PGA	0.62	0.51	1.1	0.51	1.47	0.51	1.77	0.51
	PP-band	PGA	0.48	0.53	0.86	0.53	1.15	0.53	1.39	0.53
	Steel band	PGA	0.61	0.51	1.05	0.51	1.38	0.51	1.65	0.51
Clay Bricks URM with 2 storeys MUR+CLBRH/LWAL+DNO/H:2	None (ip)	Sa(0.3s)	0.38	0.66	0.83	0.66	1.22	0.66	1.56	0.66
	None (oop)	Sa(0.3s)	–	–	–	–	–	–	0.13	1.01
	Ferrocement	Sa(0.3s)	0.75	0.57	1.54	0.57	2.23	0.57	2.84	0.57
	FRP	Sa(0.3s)	0.66	0.62	1.47	0.62	2.19	0.62	2.83	0.62
	PP-band	Sa(0.3s)	0.52	0.65	1.17	0.65	1.75	0.65	2.26	0.65
	Steel band	Sa(0.3s)	0.66	0.63	1.37	0.63	2.01	0.63	2.59	0.63
Adobe with 1 storey MUR+ADO/LWAL+DNO/H:1	None (ip)	PGA	0.3	0.59	0.45	0.59	0.57	0.59	0.67	0.59
	None (oop)	PGA	–	–	–	–	–	–	0.45	0.91
	Steel mesh	PGA	0.67	0.51	1.13	0.51	1.49	0.51	1.80	0.51
	Synthetic mesh	PGA	0.64	0.5	1.39	0.5	1.93	0.5	2.35	0.5
	Ext. steel bars	PGA	0.34	0.57	0.73	0.57	1.02	0.57	1.26	0.57
	Timber conf.	PGA	0.51	0.51	1.32	0.51	1.86	0.51	2.28	0.51
Adobe with 2 storeys MUR+ADO/LWAL+DNO/H:2	None (ip)	Sa(0.3s)	0.34	0.65	0.63	0.65	0.89	0.65	1.12	0.65
	None (oop)	Sa(0.3s)	–	–	–	–	–	–	0.49	0.95
	Steel mesh	Sa(0.3s)	0.67	0.66	1.41	0.66	2.1	0.66	2.72	0.66
	Synthetic mesh	Sa(0.3s)	0.66	0.63	1.89	0.63	2.93	0.63	3.84	0.63
	Ext. steel bars	Sa(0.3s)	0.39	0.67	1.06	0.67	1.64	0.67	2.16	0.67
	Timber conf.	Sa(0.3s)	0.51	0.66	1.86	0.66	2.96	0.66	3.91	0.66

The definition of damage limit states is often one of the most challenging steps in the derivation of fragility curves, as different interpretations may exist for each damage level. An advantage of employing thresholds linked to the yielding and ultimate spectral

displacements of the capacity curves is that the aleatory variability associated with differences in structural capacity can be explicitly accounted for. The epistemic uncertainty related to the definition of the thresholds themselves is addressed by treating each limit state probabilistically. In this approach, a probability distribution and an associated coefficient of variation are assigned to each damage limit state.

Table 4.8. Damage thresholds

Damage State	Damage Threshold
Slight	0.7 Sdy
Moderate	0.75 Sdy + 0.25 Sdu
Extensive	0.5 (Sdy + Sdu)
Collapse	Sdu

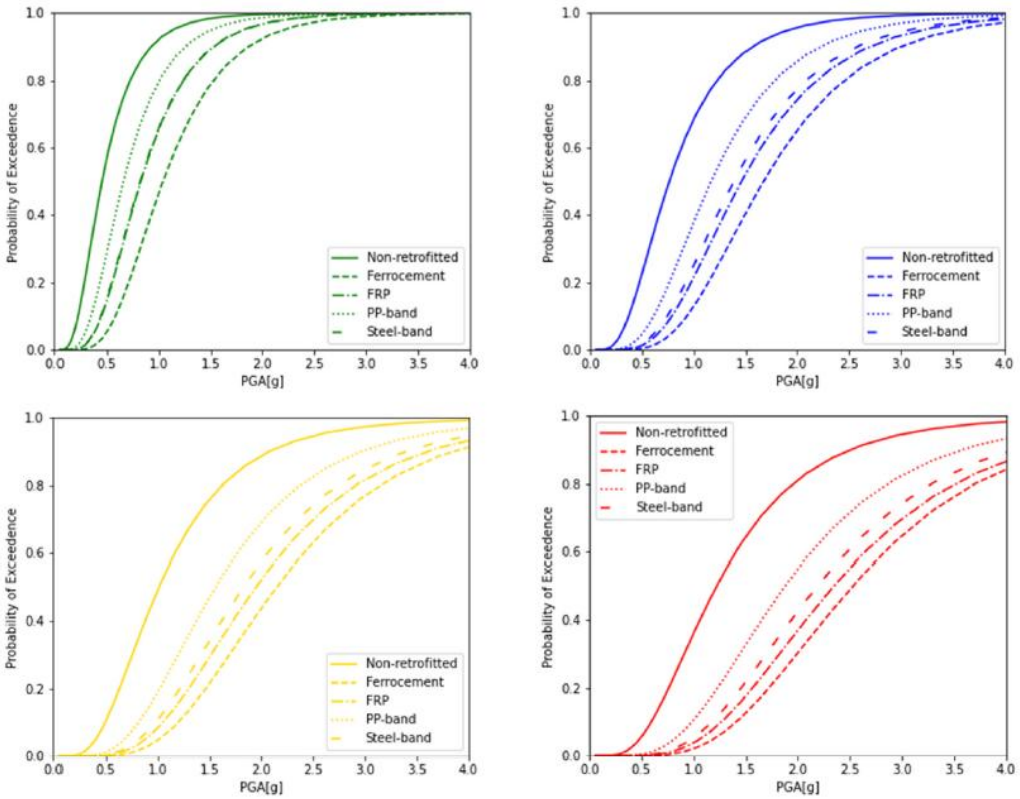


Figure 4.7 Economic value Retrofitted and non-retrofitted in-plane fragility curves for MUR+CBH/LWAL+DNO/H:1 for damage states: slight (top-left), moderate (top-right), extensive (bottom left) and collapse (bottom right).

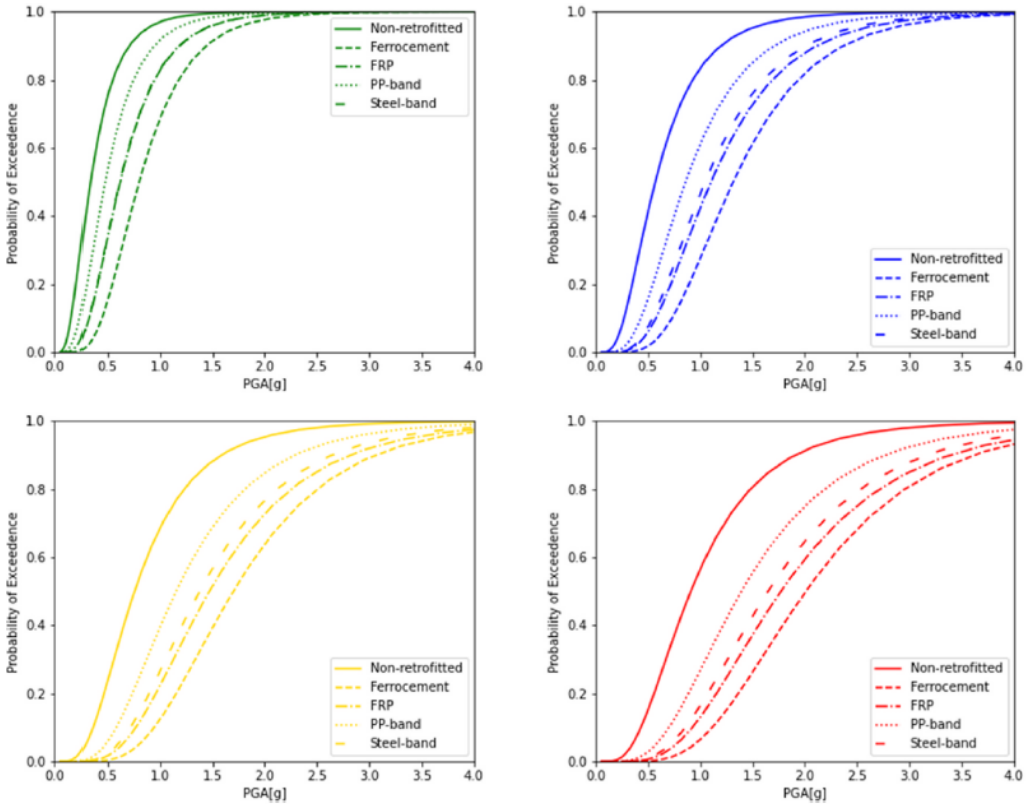


Figure 4.8 Economic Retrofitted and non-retrofitted fragility curves for MUR+CLBRH/LWAL+DNO/H:1 for damage states: slight (top-left), moderate (top-right), extensive (bottom left) and collapse (bottom right)..

It is important to note that complete damage does not necessarily imply structural collapse but rather a condition in which the damage is considered irreparable (i.e., total loss). To estimate the fraction of buildings expected to collapse, the probability of complete damage must be multiplied by a collapse rate. Estimating the number of collapsed buildings is especially important for calculating injuries and fatalities, as discussed in Section 4.3. In this study, the collapse rates proposed by Martins and Silva [2021] were adopted for the in-plane collapse of unreinforced masonry and adobe buildings.

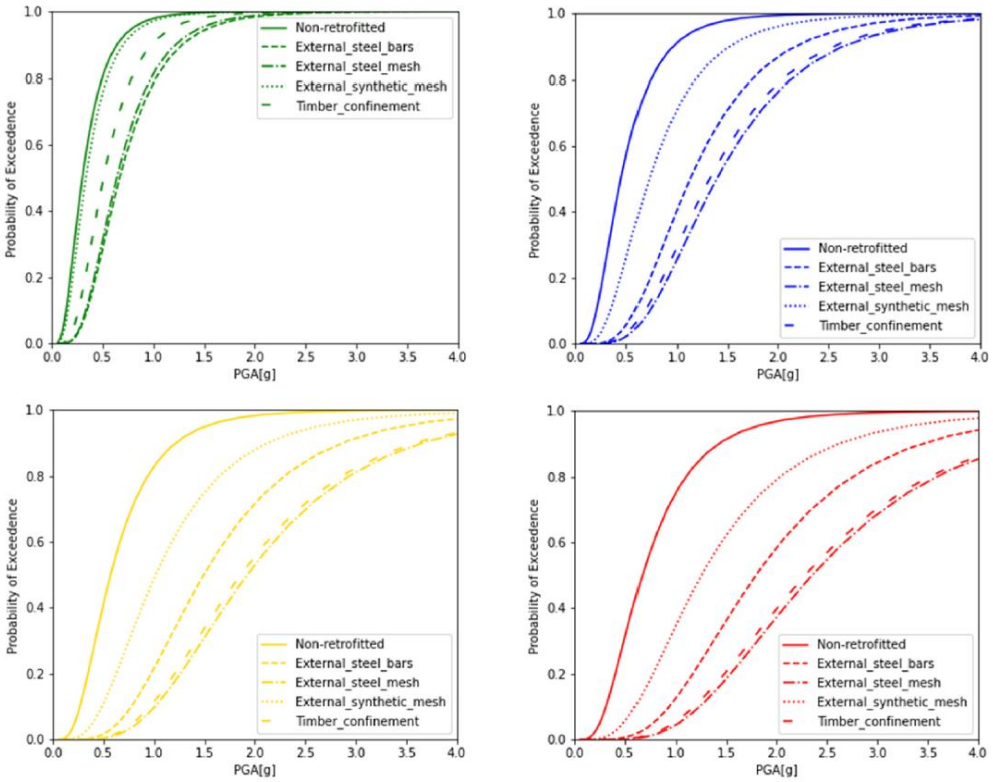


Figure 4.9 Retrofitted and non-retrofitted fragility curves for MUR+ADO/LWAL+DNO/H:1 for damage states: slight (top-left), moderate (top-right), extensive (bottom left) and collapse (bottom right).

Each fragility function is represented by a cumulative lognormal distribution, whose median and logarithmic standard deviation are presented in Table 4.2 for each building class and retrofit intervention. As examples, the fragility functions for the one-storey building typologies are shown in Figs. 4.3-4.5. A discussion of the influence of each retrofitting technique on the vulnerability of the different building classes is provided in the conclusions.

4.4 DERIVATION OF VULNERABILITY FUNCTIONS

In this study focused on the potential economic losses associated with structural damage, medical treatment of injured individuals, and monetary compensation related to fatalities. For the derivation of vulnerability functions used to estimate economic losses, the damage-to-loss model originally proposed by Yepes-Estrada and Silva [2017] for South America was adopted. This model was developed from existing methodologies implemented in Europe and the United States and subsequently calibrated using loss data from Colombia and Chile (see Table 4.4). The expected loss ratio for a given intensity measure, (E [LR | IM]), is calculated by summing the product of the probability of occurrence of each damage state, (P [DS=dsi | IM]), and its corresponding loss ratio, LR_{dsi}, as expressed in the following equation:

$$E[LR|IM] = \sum_{i=1}^{nDS} P[DS = ds_i|IM] \times LR_{ds_i} \tag{4.1}$$

Table 4.9. Parameters used for the conversion of the fragility functions into vulnerability functions for economic losses, injured and fatalities.

Damage State (ds_i)	LR | DS=ds_i	PI_3 | DS=ds_i	PI_4 | DS=ds_i	PI_5 | DS=ds_i
Slight	0.05	0.000	0.000	0.000
Moderate	0.10	0.000	0.000	0.000
Extensive	0.60	0.002	0.000	0.000
Complete	1.00	0.020	0.002	0.000
Collapse	1.00	0.090-0.200	0.005-0.050	0.070-0.100

The resulting vulnerability functions for the building classes considered herein, both with and without retrofit interventions, are presented in Fig. 4.6. The in-plane and out-of-plane failure mechanisms were combined within the vulnerability assessment using the total probability theorem. It was assumed that, provided complete in-plane damage does not occur, there remains a probability of an out-of-plane failure mechanism developing. This probability depends primarily on wall thickness and mass. Following the procedure proposed by Sumerente et al. [2020], wall thicknesses were sampled assuming the mean values reported in Table 2.1 and a coefficient of variation of 10% [Sumerente et al., 2020; Lovon et al., 2021]. This approach resulted in probabilities of out-of-plane failure of 88%, 79%, and 45% for unreinforced masonry buildings with fired-clay brick, concrete block, and adobe walls, respectively. The lower probability observed for adobe buildings is mainly due to their greater wall thickness. These probabilities were used to derive a weighted vulnerability function for each building class, except in cases where the loss ratios associated with the in-plane mechanism exceeded those associated with out-of-plane

failure. For those levels of ground shaking, the in-plane loss ratios were adopted. The inclusion of local out-of-plane failure mechanisms results in an earlier increase in mean loss ratios, even at relatively low levels of seismic intensity.

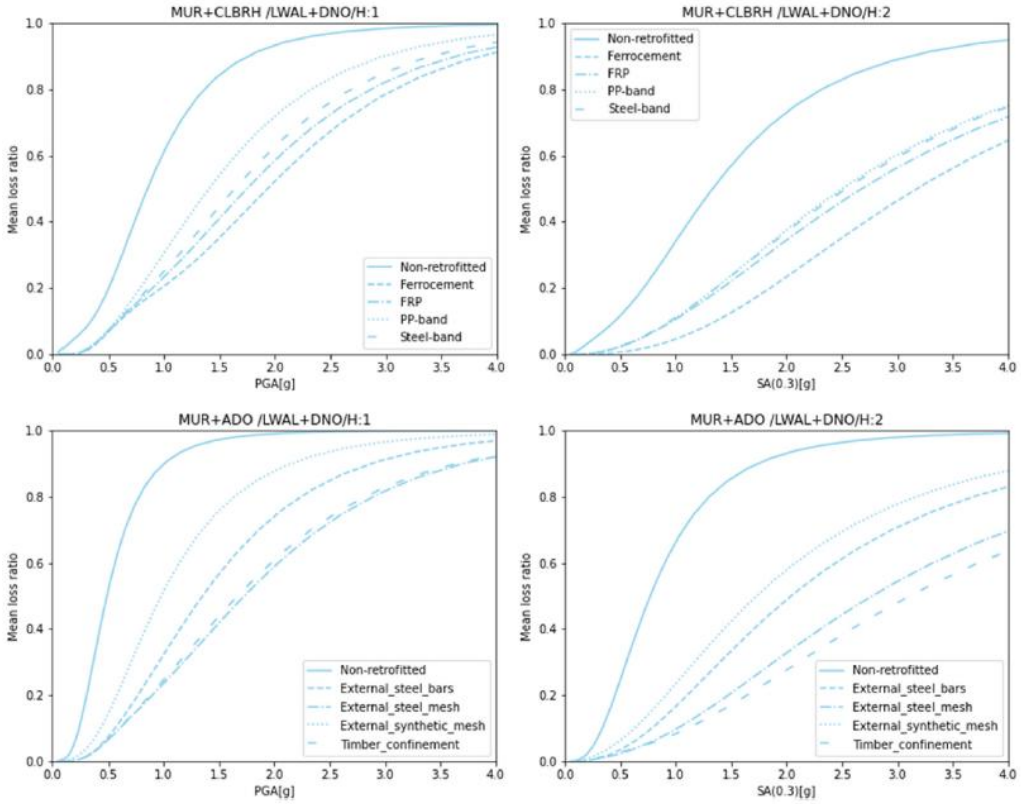


Figure 4.10 Retrofitted and non-retrofitted vulnerability curves for MUR/LWAL+DNO/H:1 (top-left), MUR/LWAL+DNO/H:2 (top-right), MUR+ADO/LWAL+DNO/H:1 (bottom-left) MUR+ADO/LWAL+DNO/H:2 (bottom-right).

For the estimation of injuries and fatalities, the injury classification proposed by Spence [2007] was adopted. This classification comprises five categories: I_1 (uninjured or lightly injured), I_2 (moderately injured), I_3 (severely injured), I_4 (critically injured), and I_5 (fatalities). According to this framework, individuals classified as I_3 and I_4 require hospitalization. It was assumed that only the last three categories contribute significantly to indirect economic losses. Vulnerability functions for injuries and fatalities were derived by multiplying the probability of each damage state by the corresponding probability of injury (PIiPI_iPIi), following the same approach used for economic losses (see Equation (4.1)). The parameters adopted for converting fragility functions into injury and fatality vulnerability functions are presented in Table 4.4. For the out-of-plane failure mechanism, only fatalities were

considered, since a single damage state was defined. The costs associated with building repair or replacement, treatment of injuries, and fatalities are described in the following section.

To estimate indirect losses associated with medical treatment, the average hospitalization duration for injury categories I_3 and I_4, together with the average daily hospital-bed cost, were determined. For critically injured individuals (I_4), it was assumed that patients are initially admitted to an intensive care unit (ICU) and subsequently transferred to a standard hospital ward once their condition stabilizes. Average hospitalization durations were assumed to be the same across the seven countries considered, while country-specific daily costs (USD) are reported in Table 4.5. Hospitalization durations for severe and critical injuries were obtained from studies analysing injury types and length of stay following earthquake events [Demirkiran et al., 2003; Li et al., 2009; Guner et al., 2013; Del Papa et al., 2019]. ICU and ward costs were compiled from general healthcare studies and publicly available sources on hospitalization costs in each country, rather than from earthquake-specific datasets.

Table 4.10. Average hospitalization time (in days) and average daily cost of injured in infirmaries or intensive care units (in USD).

Country	Average hospitalization time (days)			Average daily cost (USD)		2017 M USD	2021 M USD
	I_3	I_4					
	Infirmary	Infirmary	ICU	Infirmary	ICU		
Belize	5[i,j]	12-13[h,j]	10-12[h]	375[a]	1400[g]	0.772	0.865
Costa Rica				-	-	1.789	2.004
Guatemala				210[b]	815[b]	0.618	0.692
Honduras				200[c]	1230[c]	0.392	0.439
Nicaragua				360[d]	1110[d]	0.334	0.374
Panama				400[g]	1300[g]	2.044	2.289
El Salvador				230[f]	755[f]	0.678	0.759

a. https://belize.com/medical-care-in-belize/, b. Alvis-Guzmán et al. [2015], c. https://proceso.hn/entre-30-mil-y-150-mil-lempiras-diarios-cuesta-tener-un-paciente-en-la-uci-segun-viceministro-de-salud/, d. Alvis-Guzmán et al. [2015], e. Jara et al. [2019], f. https://www.laprensagrafica.com/elsalvador/Costo-de-una-camara-es-casi-igual-que-un-dia-en-la-uci-20171008-0060.html, g. Calculated based on values from other countries, h. Demirkiran et al. [2003] and Li et al. [2009], i. Guner et al. [2013], j. Del Papa et al. [2019].

Finally, to assign an economic value to fatalities, several studies on the value of a statistical life (VSL) were reviewed. This concept is widely used in public policy and insurance

applications, where economic valuations of mortality risk are required. In the benefit-cost analysis conducted by Liel and Deierlein [2013], a value between USD 2 million and USD 5 million per fatality was adopted based on previous studies and information from the compensation provided through the September 11th Victim Compensation Fund. Since such values are strongly country-dependent, they are not directly transferable to other regions. Viscusi and Masterman [2017] estimated VSL values for 189 countries based on local socioeconomic conditions. In this study, those values were adjusted to 2021 prices using inflation adjustments and are presented in Table 4.5.

5. BENEFIT COST ANALYSIS

A probabilistic event-based seismic risk assessment for the entire region was performed (allowing for all uncertainties to be propagated to the loss results). The analysis combined the vulnerability functions described in Section 4.4, the exposure model presented in Section 2, and the probabilistic seismic hazard model for Central America and the Caribbean developed by Garcia et al. [2018]. Average Annual Losses (AAL) were estimated using the OpenQuake engine [Silva et al., 2014], an open-source platform for seismic hazard and risk assessment. The resulting AAL values for each source of loss (i.e., structural damage, injuries, and fatalities) are presented in Fig. 5.1 for both the current building stock and the alternative retrofit interventions, assuming their implementation across the entire regional building portfolio.

The results indicate that, if the entire URM and adobe building stock in the region were retrofitted, the AAL could be reduced by more than one fifth using ferrocement for URM buildings and steel mesh or timber confinement for adobe structures. The remaining retrofit techniques also produced substantial reductions, generally ranging from one third to one half of the original losses, particularly for structural damage. When human losses are considered, the reductions could reach approximately one tenth of the original AAL. It is also worth noting that the costs associated with treating injured individuals contribute considerably less to total losses than those associated with structural damage and fatalities.

However, to establish the real benefit of the intervention, a Benefit-Cost Ratio (BCR) was calculated. The BCR represents the expected net present value of future benefits over the incurred costs of the retrofitting intervention, and it can be computed using the following expression:

$$BCR = \frac{\left(AAL_{original} - AAL_{retrofitted}\right)}{C} \frac{\left(1 - e^{-rt}\right)}{r} \tag{5.1}$$

Where $AAL_{original}$ represents the current risk, $AAL_{retrofitted}$ the risk after the implementation of a given retrofit intervention, C the retrofit cost, r the discount rate used to account for the time value of money, and t the expected service life of the building (also referred to as the time horizon, assumed herein as 50 years based on the usual assumption of life-time of engineered buildings). Regarding the discount rate, studies for Latin America based on the

gamma discounting methodology proposed by Weitzman [2001] indicate values between 4% and 5% for the evaluation of long-term projects with horizons of up to 50 years [Restrepo, 2008; Edwards, 2016; Castillo and Zhangallimbay, 2022]. Accordingly, a discount rate of 4% was adopted in the benefit-cost analysis.

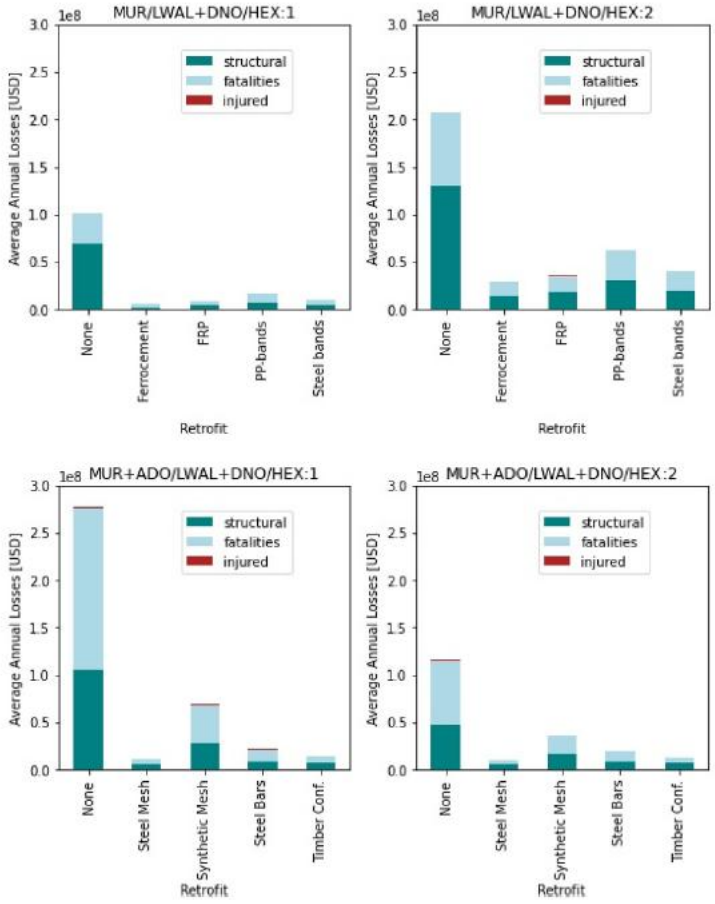


Figure 5.11. Average annual loss (AAL) in USD for the non-retrofitted and retrofitted cases

Benefit-cost analyses were performed for each retrofit technique and building class using Equation (6.1), a 50-year time horizon, and a 4% discount rate, both with and without the consideration of indirect losses (i.e., fatalities and injuries), as presented in Tables 5.1 and 5.2, respectively.

The results show that neglecting indirect losses can render many retrofit interventions economically unviable. When only structural losses are considered, benefit-cost ratios

(BCRs) greater than one are obtained only for some building classes in Guatemala, Nicaragua, and El Salvador. However, once human losses are incorporated, at least one retrofit intervention becomes economically viable in every country except Belize.

Table 5.11. BCR for the whole country considering only direct (structural) losses

Typology	Retrofit	BLZ	GTM	HND	NIC	PAN	SLV
URM with 1 storey	Ferrocement	0.04	1.31	0.41	1.77	0.62	1.35
MUR/LWAL+DNO/H:1	FRP	0.02	0.87	0.27	1.17	0.41	0.90
	PP-band	0.03	0.90	0.29	1.20	0.43	0.94
	Steel band	0.04	1.17	0.37	1.57	0.55	1.22
URM with 2 storeys	Ferrocement	0.04	0.95	0.32	1.08	0.45	0.97
MUR/LWAL+DNO/H:2	FRP	0.03	0.70	0.23	0.79	0.33	0.71
	PP-band	0.03	0.69	0.23	0.78	0.33	0.70
	Steel band	0.05	0.92	0.31	1.04	0.44	0.94
Adobe with 1 storey	Steel mesh	–	1.50	0.67	0.78	0.65	2.24
MUR+ADO/LWAL+DNO/H:1	Synthetic mesh	–	1.67	0.74	0.87	0.72	2.52
	Steel bars	–	0.96	0.42	0.50	0.41	1.45
	Timber confinement	–	1.93	0.86	1.01	0.84	2.94
Adobe with 2 storeys	Steel mesh	–	1.02	0.43	0.6	–	1.39
MUR+ADO/LWAL+DNO/H:2	Synthetic mesh	–	0.10	0.04	0.06	–	0.14
	Steel bars	–	0.64	0.26	0.38	–	0.89
	Timber confinement	–	1.20	0.50	0.70	–	1.66

Table 5.12. BCR for the whole country considering direct and indirect (fatalities and injuries)

Typology	Retrofit	BLZ	GTM	HND	NIC	PAN	SLV
URM with 1 storey	Ferrocement	0.05	3.26	0.70	2.96	2.08	3.01
MUR/LWAL+DNO/H:1	FRP	0.04	2.30	0.49	2.03	1.48	2.13
	PP-band	0.04	2.43	0.52	2.13	1.59	2.25
	Steel band	0.05	3.06	0.66	2.72	1.98	2.85
URM with 2 storeys	Ferrocement	0.05	2.21	0.52	1.73	1.41	2.02
MUR/LWAL+DNO/H:2	FRP	0.03	1.72	0.39	1.32	1.10	1.56
	PP-band	0.04	1.70	0.40	1.30	1.10	1.55
	Steel band	0.05	2.23	0.52	1.73	1.44	2.04
Adobe with 1 storey	Steel mesh	–	4.38	1.33	1.41	2.62	6.04
MUR+ADO/LWAL+DNO/H:1	Synthetic mesh	–	4.95	1.49	1.59	2.95	6.85
	Steel bars	–	3.25	0.96	1.01	2.01	4.45
	Timber confinement	–	5.62	1.71	1.83	3.36	7.82
Adobe with 2 storeys	Steel mesh	–	2.83	0.83	1.06	–	3.51
MUR+ADO/LWAL+DNO/H:2	Synthetic mesh	–	0.40	0.11	0.13	–	0.48
	Steel bars	–	2.12	0.59	0.75	–	2.61
	Timber confinement	–	3.59	1.01	1.31	–	4.46

losses.

A further analysis was conducted at a lower administrative level within each country to identify areas where retrofit investments may be economically advantageous. Figures 5.2-5.5 present the BCR of the most favourable retrofit intervention for unreinforced masonry and adobe buildings, with and without consideration of indirect losses. Figures 5.6 and 5.7 indicate the most economically viable retrofit technique, where applicable.

These results indicate that retrofitting adobe structures generally yields higher BCRs than retrofitting unreinforced masonry buildings. It is also noteworthy that retrofit interventions appear to be more economically attractive in the western regions of the countries considered, whereas they become less viable toward the east. This spatial pattern is largely

driven by the regional distribution of seismic hazard, which is highest in the western part of the study area, where peak ground acceleration (PGA) on rock for a 475-year return period exceeds 0.3 g.

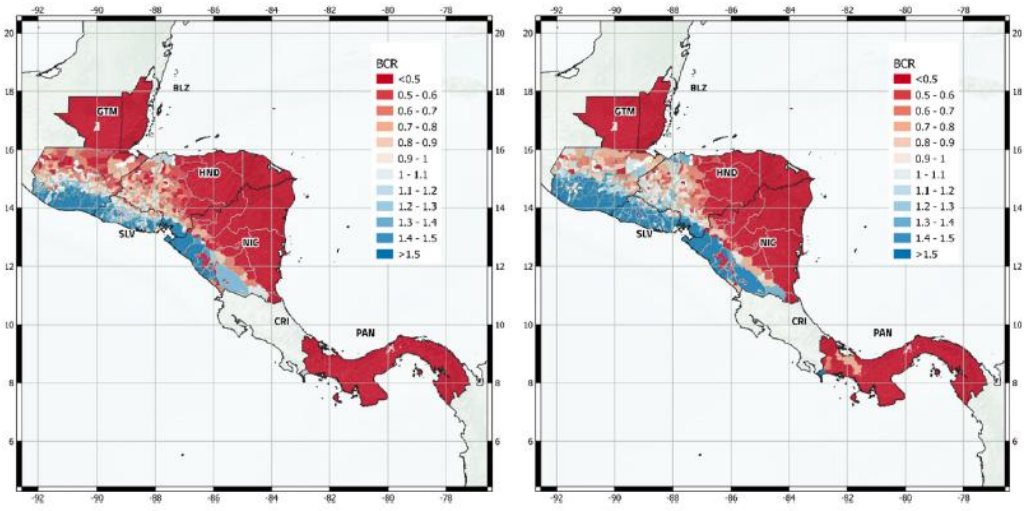


Figure 5.12 **Highest Benefit Cost Ratio (BCR) at sub-national level in Central America for 1-storey unreinforced masonry, considering only direct losses [left], and considering the total losses [right].**

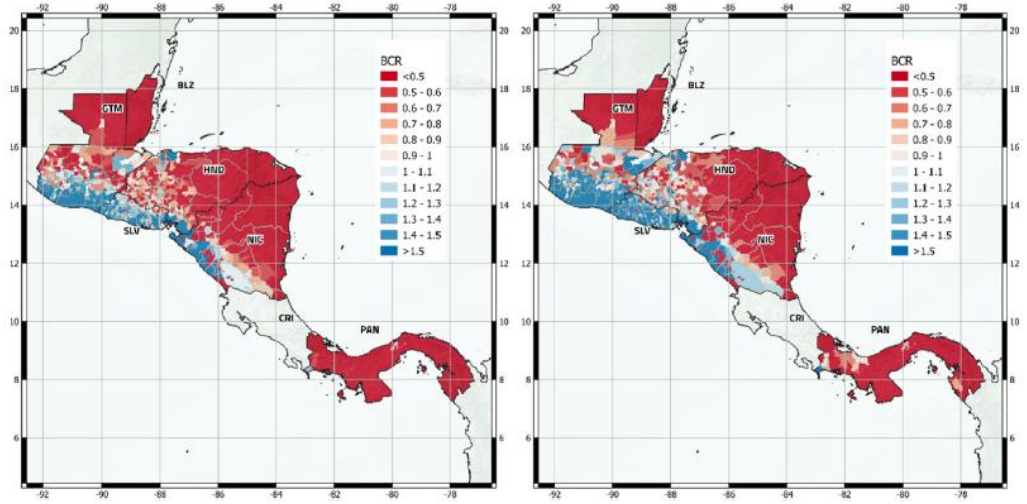


Figure 5.13 **Highest Benefit Cost Ratio (BCR) at sub-national level in Central America for 2-storey unreinforced masonry, considering only direct losses [left], and considering the total losses [right].**

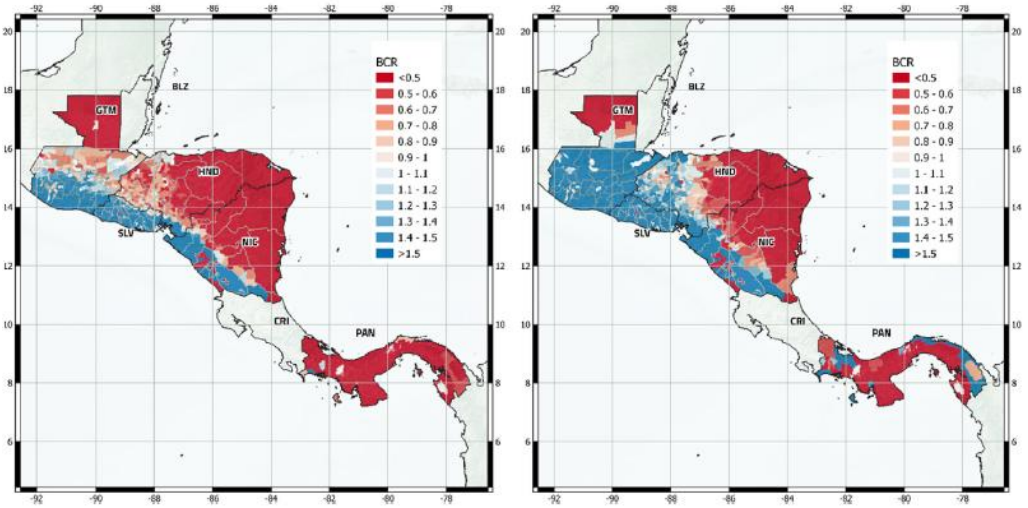


Figure 5.14 Highest Benefit Cost Ratio (BCR) at sub-national level in Central America for 1-storey adobe, considering only direct losses [left], and considering the total losses [right].

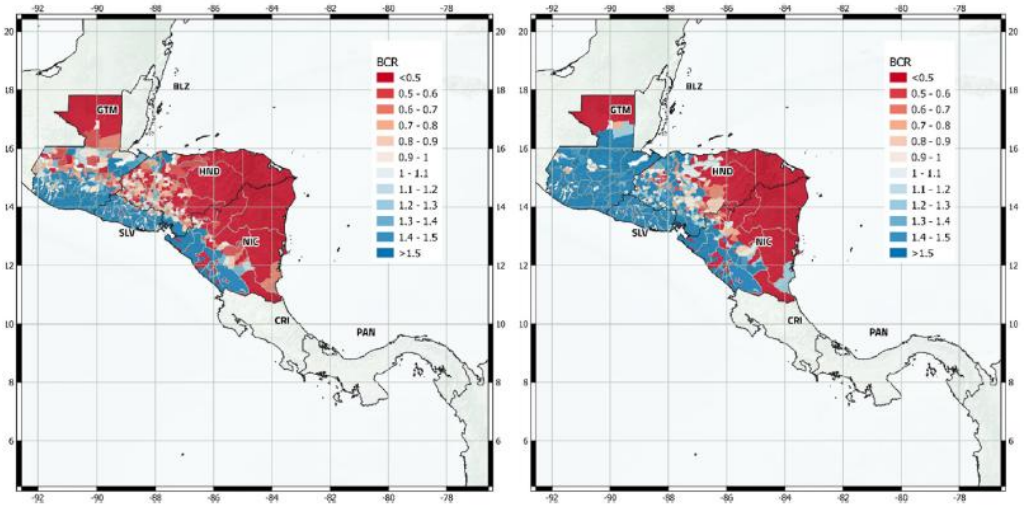


Figure 5.15 Highest Benefit Cost Ratio (BCR) at sub-national level in Central America for 2-storey adobe, considering only direct losses [left], and considering the total losses [right].

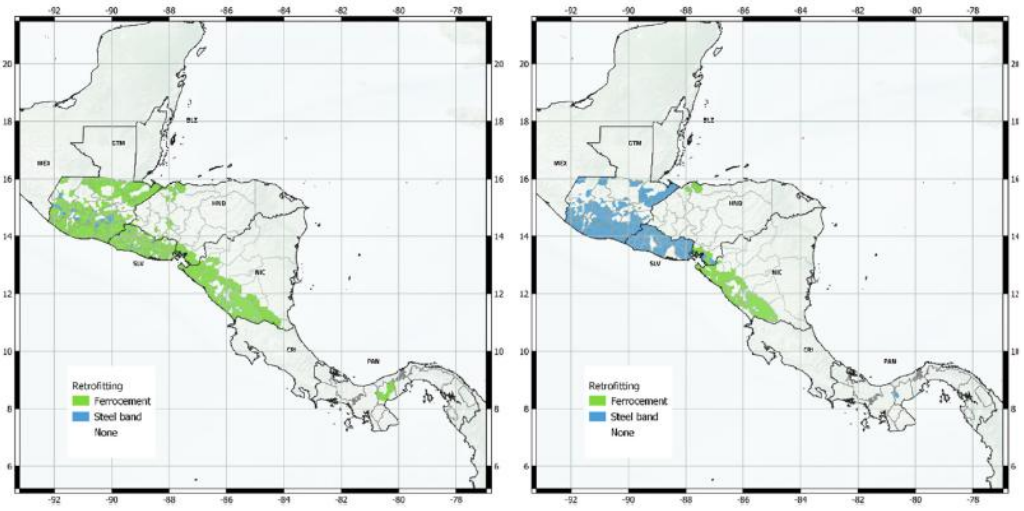


Figure 5.16 Optimal retrofitting technique (technique with highest BCR ratio when BCR>1) for the 1-storey URM (left) and the 2-storey URM (right) residential building stock.

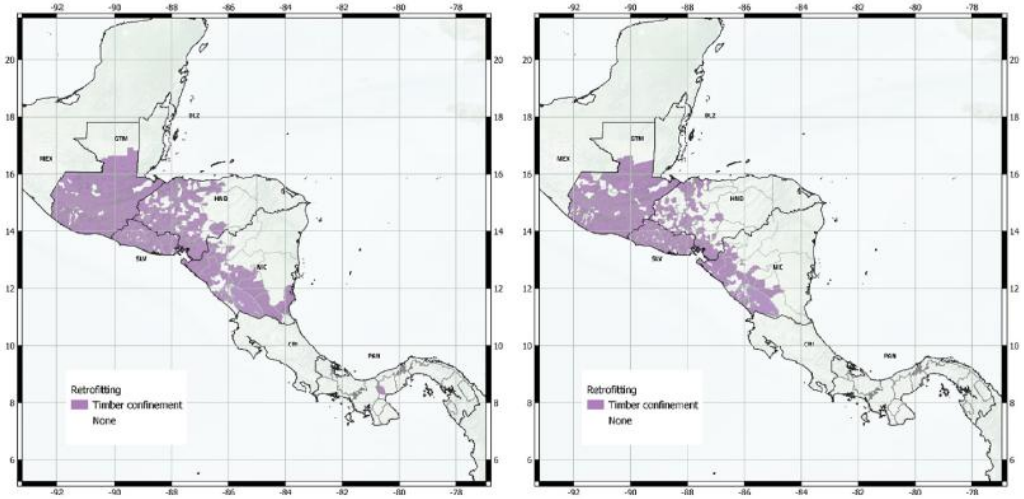


Figure 5.17 Optimal retrofitting technique (technique with highest BCR ratio when BCR>1) for the 1- storey adobe (left) and 2-storey adobe (right) residential building stock.

6. CONCLUSIONS

This study presented a methodology to evaluate the economic viability of retrofit interventions by considering potential losses arising from structural damage, injury treatment, and the statistical value of human life. The framework was applied to the unreinforced masonry and adobe building stock of Central America. The review of existing retrofit techniques identified several interventions that have been extensively tested in the region, including the application of external steel meshes, timber confinement, and polymer or steel bands. These techniques have demonstrated significant potential to reduce both the probability of structural damage (see Figs. 4.3-4.5) and the resulting economic losses (see Fig. 4.6). Fragility and vulnerability functions were developed for each intervention, enabling their future application and further exploration by the broader research and engineering community.

The probabilistic seismic loss assessment is consistent with previous studies [UNDRR, 2015; Calderón et al., 2021; World Bank Group, 2017], which indicate moderate-to-high seismic risk across much of Central America, particularly in Guatemala, Nicaragua, and El Salvador. The benefits of retrofit interventions were evaluated considering three sources of loss. Similar to the findings of Liel and Deierlein [2013] for California, the results suggest that reductions in structural damage alone are generally insufficient to justify retrofit investments from an economic perspective, unless seismic hazard levels are exceptionally high. To address this limitation, the analysis incorporated the savings associated with reductions in injuries and fatalities, which substantially increased the resulting benefit-cost ratios (see Tables 5.1 and 5.2). Nevertheless, the contribution of injury-treatment costs was found to be negligible when compared with the statistical value assigned to human life.

The results indicate that structural retrofitting can be economically viable in Guatemala, Nicaragua, El Salvador, Honduras, and in some areas of central Panama. In contrast, such interventions are generally less attractive in Belize and most parts of Panama due to their comparatively lower seismic hazard. According to Calderón et al. [2021], the seismic hazard, expressed as PGA on rock for a 475-year return period, is approximately 0.25 g in

Panama City and 0.12 g in Belize City, substantially lower than the values exceeding 0.5 g observed in the remaining Central American capitals. The influence of seismic hazard is also evident within individual countries, with benefit-cost ratios typically exceeding one in western regions located closer to the subduction zone, where hazard levels are highest.

From a purely economic standpoint, ferrocement and steel bands emerged as the most advantageous retrofit solutions for unreinforced masonry buildings, while timber confinement was identified as the most favourable option for adobe structures. The implementation of these interventions has the potential to reduce economic losses by up to one fifth and human losses by up to one tenth. Such substantial reductions in seismic risk could support progress toward the objectives of both the Sendai Framework for Disaster Risk Reduction and the United Nations Sustainable Development Goals. However, it is unrealistic to assume that an entire national building stock can be retrofitted, regardless of the resources available. Given the limited funds typically allocated to risk-reduction programmes, it is essential to identify both the interventions that maximise the benefits of those resources and the regions where they should be prioritised. The results presented herein provide information that can support decision-makers in addressing these challenges.

REFERENCES

Weesjes, E. [2016] "Constructed catastrophe, the age-old tale of less quake, more damage," Natural Hazards Center, University of Colorado Boulder, USA.

Silva, V., Amo-Oduro, D., Calderón, A., Costa, C., Dabbeek, J., Despotaki, V., Martins, L., Pagani, M., Rao, A., Simionato, M., Viganò, D., Yepes-Estrada, C., Acevedo, A., Crowley, H., Horspool, N., Jaiswal, K., Journeay, M. and Pittore, M. [2020] "Development of a global seismic risk model," Earthquake Spectra.

Kappos, A.J. and Dimitrakopoulos, E.G. [2008] "Feasibility of pre-earthquake strengthening of buildings based on cost-benefit and life-cycle cost analysis, with the aid of fragility curves," Natural Hazards, 45(1), pp. 33-54.

Liel, A.B. and Deierlein, G.G. [2013] "Cost-benefit evaluation of seismic risk mitigation alternatives for older concrete frame buildings," Earthquake Spectra, 29(4), pp. 1391-1411.

Pomonis, A. and Gaspari, M. [2013] "Earthquake loss estimation and benefit-cost analysis of mitigation measures for buildings in Greece: case study of Pylos town," Bollettino di Geofisica Teorica ed Applicata, 54.

Valcárcel, J.A., Mora, M.G., Cardona, O.D., Pujades, L.G., Barbat, A.H. and Bernal, G.A. [2013] "Methodology and applications for the benefit-cost analysis of the seismic risk reduction in building portfolios at broad scale," Natural Hazards, 69(1), pp. 845-868.

Jaimes, M.A. and Niño, M. [2017] "Cost-benefit analysis to assess seismic mitigation options in Mexican public school buildings," Bulletin of Earthquake Engineering, 15(9), pp. 3919-3942.

Giordano, N., Crespi, P. and Franchi, A. [2018] "Cost-benefit analysis for the retrofit of masonry buildings through performance-based seismic assessment," Proceedings of the 10th International Masonry Conference, Milan, Italy, pp. 982-990.

Cardone, D., Gesualdi, G. and Perrone, G. [2019] "Cost-benefit analysis of alternative retrofit strategies for RC frame buildings," Journal of Earthquake Engineering, 23(2), pp. 208-241.

Vitiello, U., Asprone, D., Di Ludovico, M. and Prota, A. [2017] "Life-cycle cost optimization of the seismic retrofit of existing RC structures," Bulletin of Earthquake Engineering, 15(5), pp. 2245-2271.

Dumaru, R., Rodrigues, H. and Varum, H. [2019] "Cost-benefit analysis of retrofitted non-engineered and engineered buildings in Nepal using probabilistic approach," Soil Dynamics and Earthquake Engineering, 122, pp. 1-15.

Giordano, N., Norris, A., Manandhar, V., Shrestha, L., Paudel, D.R., Quinn, N. and Luca, A.S. [2020] "Life-cycle analysis of incremental seismic retrofitting of traditional constructions in Nepal."

Calderón, A., Silva, V., Avilés, M., Méndez, R., Castillo, R., Gil, J.C. and López, M.A. [2021] "Toward a uniform earthquake loss model across Central America," Earthquake Spectra.

Silva, V., Brzev, S., Scawthorn, C., Yepes-Estrada, C., Dabbeek, J. and Crowley, H. [2022] "A building classification system for multi-hazard risk assessment," International Journal of Disaster Risk Science.

Costa, A.C., Sousa, M.L., Carvalho, A. and Coelho, E. [2010] "Evaluation of seismic risk and mitigation strategies for the existing building stock: application of LNECloss to the metropolitan area of Lisbon," Bulletin of Earthquake Engineering, 8(1), pp. 119-134.

Martins, L. and Silva, V. [2021] "Development of a fragility and vulnerability model for global seismic risk analyses," Bulletin of Earthquake Engineering, 19(15), pp. 6719-6745.

Daniell, J.E. [2014] "The socioeconomic impact of earthquake disasters," in Shroder, J. (Ed.), Earthquake Hazard, Risk and Disasters, Amsterdam, Netherlands, pp. 203-236.

ElGawady, M., Lestuzzi, P. and Badoux, M. [2004] "A review of conventional seismic retrofitting techniques for URM," Proceedings of the 13th International Brick and Block Masonry Conference, Amsterdam, Netherlands, pp. 1-10.

Smith, A. and Redman, T. [2009] "A critical review of retrofitting methods for unreinforced masonry structures," Proceedings of the EWB-UK Research Conference, Royal Academy of Engineering, United Kingdom.

Sathiparan, N. [2015] "Mesh type seismic retrofitting for masonry structures: critical issues and possible strategies," European Journal of Environmental and Civil Engineering, 19(9), pp. 1136-1154.

Dadras Eslamlou, S., Masia, M.J., Totoev, Y.Z. and Page, A.W. [2019] "Effect of retrofitting on the structural factors for seismic assessment of unreinforced masonry structures: a review," Australian Journal of Structural Engineering, 20(1), pp. 26-53.

Ashraf, M., Khan, A.N., Naseer, A., Ali, Q. and Alam, B. [2012] "Seismic behavior of unreinforced and confined brick masonry walls before and after ferrocement overlay retrofitting," International Journal of Architectural Heritage, 6(6), pp. 665-688.

Nayak, S. and Dutta, S.C. [2016] "Failure of masonry structures in earthquake: a few simple cost-effective techniques as possible solutions," Engineering Structures, 106, pp. 53-67.

Abrams, D., Smith, T., Lynch, J. and Franklin, S. [2007] "Effectiveness of rehabilitation on seismic behavior of masonry piers," Journal of Structural Engineering, 133(1), pp. 32-43.

Ahmad, Z., Shahzada, K., Gencturk, B., Khan, A.N., Rehan, R., Fahad, M. and Ali, Z. [2015] "Seismic capacity assessment of unreinforced concrete block masonry buildings in Pakistan before and after retrofitting," Journal of Earthquake Engineering, 19(3), pp. 357-382.

Villalba, P., Sánchez-Garrido, A. J., Yepes-Bellver, L., & Yepes, V. [2025]. A Hybrid Fuzzy DEMATEL–DANP–TOPSIS Framework for Life Cycle-Based Sustainable Retrofit Decision-Making in Seismic RC Structures. Mathematics, 13(16), 2649.

Khursheed, S., Upasani, S., & Paul, V. K. [2024]. Comparative cost-benefit analysis of carbon wrapping and concrete jacketing for seismic retrofitting of RCC hospital buildings. International Journal of Applied Systemic Studies, 11(4), 298-310.Abrahamson, N.A., Silva, W.J. [1997] "Empirical response spectral attenuation relations for shallow crustal earthquakes," *Seismological Research Letters*; Vol. 68, No. 1, pp. 94-127.

Aljawhari, K., Gentile, R., & Galasso, C. [2025]. Beyond direct economic losses: an integrated approach to seismic retrofit considering sustainability and indirect losses. *Earthquake Engineering & Structural Dynamics*, *54*(6), 1737-1758.

Shabdin, M., Attari, N.K.A. and Zargaran, M. [2019] "Experimental study on seismic behavior of unreinforced masonry (URM) brick walls strengthened in the boundaries with shotcrete," Journal of Earthquake Engineering.

López, S., Quiroga, P.N. and Torres, N. [2013] "Evaluación analítica y experimental de muros de mampostería no reforzada y reforzada externamente con mortero y malla electrosoldada," Proceedings of the VI Congreso Nacional de Ingeniería Sísmica, Bucaramanga, Colombia.

Sandoval, O.J., Takeuchi, C., Carrillo, J. and Barahona, B. [2021] "Performance of unreinforced masonry panels strengthened with mortar overlays reinforced with welded wire mesh and transverse connectors," Construction and Building Materials, 267, 121054.

Marcari, G., Manfredi, G., Prota, A. and Pecce, M. [2007] "In-plane shear performance of masonry panels strengthened with FRP," Composites Part B: Engineering, 38(7), pp. 887-901.

Alcaíno, P. and Santa María, H. [2008] "Resistencia al corte de muros de albañilería reforzados exteriormente con fibras," Proceedings of the XXXIII Jornadas Sudamericanas de Ingeniería Estructural, Santiago, Chile.

San Bartolomé, A. and Coronel, C. [2011] "Reparación y reforzamiento de un muro de albañilería confinada mediante fibra de carbono," Pontificia Universidad Católica del Perú, Peru.

Ramírez de Alba, H. and Carreón Guardado, B. [2004] "Experimental study on masonry walls strengthened with steel and plastic straps," Proceedings of the 13th World Conference on Earthquake Engineering, Vancouver, Canada.

Arias, A. and López, E. [2018] "Análisis comparativo de muros de mampostería reforzada con y sin fibra de carbono," Undergraduate Dissertation, Tecnológico de Costa Rica, Costa Rica.

Mayorca, P. and Meguro, K. [2004] "Proposal of an efficient technique for retrofitting unreinforced masonry dwellings," Proceedings of the 13th World Conference on Earthquake Engineering, Vancouver, Canada.

Banerjee, S., Nayak, S. and Das, S. [2019] "Enhancing the flexural behaviour of masonry wallets using PP band and steel wire mesh," Construction and Building Materials, 194, pp. 179-191.

Farooq, S.H., Ilyas, M. and Ghaffar, A. [2006] "Technique for strengthening of masonry wall panels using steel strips," Asian Journal of Civil Engineering, 7(6), pp. 621-638.

Farooq, S.H., ElGawady, M.A. and Ilyas, M. [2014] "Seismic in-plane performance of retrofitted masonry walls," KSCE Journal of Civil Engineering, 18(1), pp. 226-237.

Ahumada Forero, G. [2015] "Reforzamiento y rehabilitación de fachadas de mampostería construidas en Bogotá D.C., Colombia, antes de la expedición del reglamento NSR-10," Doctoral Dissertation, Universidad Nacional de Colombia, Colombia.

Daniell, J.E. and Schäfer, A. [2014] "Making an Australian brick house more earthquake-resistant for $100 or less: ideas, practice and loss analysis," Proceedings of the Australian Earthquake Engineering Society Conference, Lorne, Australia.

Build Change and AGIES [2019] "Manual de evaluación sísmica y reforzamiento simplificado de viviendas en mampostería de block en Guatemala," Technical Manual, Guatemala.

Anwar, N., Adhikari, S., Shahid, M. and Shrestha, S. [2016] "Making schools safer for earthquakes: effectiveness of retrofitting, case studies from Nepal," Asian Institute of Technology, Thailand.

Kadam, S.B., Singh, Y. and Li, B. [2015] "Out-of-plane behaviour of unreinforced masonry strengthened using ferrocement overlay," Materials and Structures, 48(10), pp. 3187-3203.

Baena, J.F. [n.d.] "Evaluación experimental de la respuesta fuera del plano de muros de mampostería no reforzada y reforzada con franjas de mallas electrosoldadas y mortero," Master's Dissertation, Universidad EAFIT, Medellín, Colombia.

Mahmood, H. and Ingham, J.M. [2011] "Diagonal compression testing of FRP-retrofitted unreinforced clay brick masonry wallettes," Journal of Composites for Construction, 15(5), pp. 810-820.

Hoeppner, C.R., Sparling, B.F., Wegner, L.D. and Sakr, K. [2002] "CFRP reinforced masonry walls subjected to out-of-plane loading," Proceedings of the 4th Structural Specialty Conference of the Canadian Society for Civil Engineering, Montreal, Canada.

Tan, K.H. and Patoary, M.K.H. [2004] "Strengthening of masonry walls against out-of-plane loads using fiber-reinforced polymer reinforcement," Journal of Composites for Construction, 8(1), pp. 79-87.

Sathiparan, N. [2020] "State-of-the-art review on PP-band retrofitting for masonry structures," Innovative Infrastructure Solutions, 5(2).

Varum, H., Tarque, N., Silveira, D., Camata, G., Lobo, B., Blondet, M. and Costa, A. [2014] "Structural behaviour and retrofitting of adobe masonry buildings," in Structural Rehabilitation of Old Buildings, Springer, Berlin, Germany, pp. 37-75.

Dowling, D.M. [2004] "Adobe housing in El Salvador: earthquake performance and seismic improvement," Geological Society of America Special Papers, pp. 281-300.

Illampas, R., Ioannou, I. and Charmpis, D.C. [2013] "Overview of the pathology, repair and strengthening of adobe structures," International Journal of Architectural Heritage, 7(2), pp. 165-188.

Vargas-Neumann, J., Oliveira, C., Silveira, D. and Varum, H. [2018] "Seismic retrofit of adobe constructions," in Strengthening and Retrofitting of Existing Structures, Springer, Singapore, pp. 85-111.

Herrera, R.G., Carboney, J.A. and Soberón, C.G. [2008] "Vulnerabilidad de viviendas de adobe en Chiapas y alternativas de reparación," Proceedings of the XVI Congreso Nacional de Ingeniería Estructural, Veracruz, Mexico.

Yamín Lacouture, L.E., Phillips Bernal, C., Ortiz, R. and Ruiz Valencia, D. [2007] "Estudios de vulnerabilidad sísmica, rehabilitación y refuerzo de casas en adobe y tapia pisada," Apuntes: Revista de Estudios sobre Patrimonio Cultural, 20(2), pp. 286-303.

Reyes, J.C., Smith-Pardo, J.P., Yamín, L.E., Galvis, F.A., Angel, C.C., Sandoval, J.D. and Gonzalez, C.D. [2019] "Seismic experimental assessment of steel and synthetic meshes for retrofitting heritage earthen structures," Engineering Structures, 198, 109477.

Oliveira, C., Varum, H., Figueiredo, A., Silveira, D. and Costa, A. [2010] "Experimental tests for seismic assessment and strengthening of adobe structures," Proceedings of the 14th European Conference on Earthquake Engineering, Ohrid, Republic of Macedonia.

Torrealva, D. [2012] "Seismic design criteria for adobe buildings reinforced with geogrids," Proceedings of the 15th World Conference on Earthquake Engineering, Lisbon, Portugal.

Figueiredo, A., Varum, H., Costa, A., Silveira, D. and Oliveira, C. [2013] "Seismic retrofitting solution of an adobe masonry wall," Materials and Structures, 46(1), pp. 203-219.

Banadaki, H.M., Morshed, R. and Eslami, A. [2019] "In-plane cyclic performance of adobe walls retrofitted with near-surface-mounted steel rebars," Engineering Structures, 194, pp. 106-119.

Reyes, J.C., Smith-Pardo, J.P., Yamín, L.E., Galvis, F.A., Sandoval, J.D., Gonzalez, C.D. and Correal, J.F. [2019] "In-plane seismic behavior of full-scale earthen walls with openings retrofitted with timber elements and vertical tensors," Bulletin of Earthquake Engineering.

Dowling, D. [2006] "Seismic Strengthening of Adobe-Mudbrick Houses," Doctoral Dissertation, University of Technology Sydney, Australia.

San Bartolome, A., Quiun, D. and Zegarra, L. [2008] "Performance of reinforced adobe houses in the Pisco, Peru earthquake," Proceedings of the 14th World Conference on Earthquake Engineering, Beijing, China.

CERESIS [2015] "Manual técnico para el reforzamiento de las viviendas de adobe existentes en la Costa y Sierra," Technical Manual, Proyecto Adobe, Peru.

JICA [2010] "Seeking Earthquake Resistant Housing," TAISHIN Project, La Prensa Gráfica, El Salvador.

FUNDASAL [2014] "Construcción y rehabilitación de viviendas de adobe para el desarrollo del hábitat rural: caso Proyecto El Pinalito," Proceedings of the 14 SIACOT, Arquitectura de Tierra: Patrimonio y Sustentabilidad en Regiones Sísmicas, Red Proterra.

Torrealva, D., Cerrón, C. and Espinoza, Y. [2008] "Shear and out-of-plane bending strength of adobe walls externally reinforced with polypropylene grids," Proceedings of the 14th World Conference on Earthquake Engineering, Beijing, China.

Ruiz, D., López, C., Unigarro, S. and Domínguez, M. [2014] "Seismic rehabilitation of sixteenth- and seventeenth-century rammed-earth churches in the Andean Highlands: field and laboratory study," Journal of Performance of Constructed Facilities, 29(6).

Yamín, L.E., Phillips, C.A., Reyes, J.C. and Ruiz, D.M. [2004] "Seismic behavior and rehabilitation alternatives for adobe and rammed-earth buildings," Proceedings of the 13th World Conference on Earthquake Engineering, Vancouver, Canada.

Yamín, L.E., Rodríguez, A.E., Fonseca, L.R., Reyes, J.C. and Phillips, C.A. [2003] "Comportamiento sísmico y alternativas de rehabilitación de edificaciones en adobe y tapia pisada con base en modelos a escala reducida ensayados en mesa vibratoria," Revista de Ingeniería, 18, pp. 175-190.

Martins, L., Silva, V., Crowley, H. and Cavalieri, F. [2021] "Vulnerability Modeller's Toolkit: an open-source platform for vulnerability analysis," Bulletin of Earthquake Engineering, 19(13), pp. 5691-5709.

Jalayer, F., De Risi, R. and Manfredi, G. [2015] "Bayesian cloud analysis: efficient structural fragility assessment using linear regression," Bulletin of Earthquake Engineering, 13(4), pp. 1183-1203.

Akkar, S., Sucuoglu, H. and Yakut, A. [2005] "Displacement-based fragility functions for low- and mid-rise ordinary concrete buildings," Earthquake Spectra, 21(4), pp. 901-927.

Erberik, M.A. [2008] "Fragility-based assessment of typical mid-rise and low-rise RC buildings in Turkey," Engineering Structures, 30(5), pp. 1360-1374.

Suzuki, A. and Iervolino, I. [2019] "Seismic fragility of code-conforming Italian buildings based on SDOF approximation," Journal of Earthquake Engineering.

Villar-Vega, M., Silva, V., Crowley, H., Yepes, C., Tarque, N., Acevedo, A. and Hube, M. [2017] "Development of a fragility model for the residential building stock in South America," Earthquake Spectra, 33(2), pp. 581-604.

Doherty, K., Griffith, M.C., Lam, N. and Wilson, J. [2002] "Displacement-based seismic analysis for out-of-plane bending of unreinforced masonry walls," Earthquake Engineering and Structural Dynamics, 31(4), pp. 833-850.

Sumerente, G., Lovon, H., Tarque, N. and Chácara, C. [2020] "Assessment of combined in-plane and out-of-plane fragility functions for adobe masonry buildings in the Peruvian Andes," Frontiers in Built Environment, 6, 52.

Federal Emergency Management Agency (FEMA) [2004] Using HAZUS-MH for Risk Assessment (FEMA 433), Federal Emergency Management Agency, Washington, DC, USA.

Borzi, B., Crowley, H. and Pinho, R. [2008] "Simplified pushover-based earthquake loss assessment (SP-BELA) method for masonry buildings," International Journal of Architectural Heritage, pp. 353-376.

Yepes-Estrada, C. and Silva, V. [2017] "Probabilistic seismic risk assessment of the residential building stock in South America," Proceedings of the 16th World Conference on Earthquake Engineering, Santiago, Chile.

Lovon, H., Silva, V., Vicente, R., Ferreira, T.M. and Costa, A.A. [2021] "Characterisation of the masonry building stock in Portugal for earthquake risk assessment," Engineering Structures, 233

Spence, R. (Ed.) [2007] Earthquake Disaster Scenario Predictions and Loss Modelling for Urban Areas, IUSS Press, Pavia, Italy.

Demirkiran, O., Dikmen, Y., Utku, T. and Urkmez, S. [2003] "Crush syndrome patients after the Marmara earthquake," Emergency Medicine Journal, 20(3), pp. 247-250.

Li, W., Qian, J., Liu, X., Zhang, Q., Wang, L., Chen, D. and Lin, Z. [2009] "Management of severe crush injury in a front-line tent ICU after the 2008 Wenchuan earthquake in China: an experience with 32 cases," Critical Care, 13(6).

Guner, S., Guner, S.I., Isik, Y., Gormeli, G., Kalender, A.M., Turktas, U. and Dursun, R. [2013] "Review of Van earthquakes from an orthopaedic perspective: a multicentre retrospective study," International Orthopaedics, 37(1), pp. 119-124.

Del Papa, J., Vittorini, P., D'Aloisio, F., Muselli, M., Giuliani, A.R., Mascitelli, A. and Fabiani, L. [2019] "Retrospective analysis of injuries and hospitalizations of patients following the 2009 earthquake of L'Aquila City," International Journal of Environmental Research and Public Health, 16(10), 1675.

Alvis-Guzman, N., Castañeda-Orjuela, C., Carrasquilla-Sotomayor, M., Sanchez-Ruiz, C., Mena, R. and Marin-Correa, C. [2015] "Costos de hospitalización por infección respiratoria aguda grave (IRAG) en Guatemala," Value in Health, 18(7), A870.

Alvis-Guzmán, N., Marín-Correa, C., Castañeda-Orjuela, C., Sánchez-Ruiz, C., Largaespada, J.F.S. and Carrasquilla-Sotomayor, M. [2015] "Costos de tratamiento hospitalario de la infección respiratoria aguda grave en niños de Nicaragua," Infectio, 19(4), pp. 144-149.

Jara, J.H., Azziz-Baumgartner, E., De Leon, T., Luciani, K., Brizuela, Y.S., Estripeaut, D. and Dawood, F.S. [2019] "Costs associated with acute respiratory illness and select virus infections in hospitalized children, El Salvador and Panama, 2012-2013," Journal of Infection, 79(2), pp. 108-114.

Viscusi, W.K. and Masterman, C.J. [2017] "Income elasticities and global values of a statistical life," Journal of Benefit-Cost Analysis, 8(2), pp. 226-250.

Garcia, J., Pagani, M., Gee, R., Poggi, V., Styron, R. and Johnson, K. [2018] "Assessing earthquake hazard in the Caribbean and Central America within the CCARA project," Proceedings of the Seismology of the Americas Meeting, Miami, USA.

Silva, V., Crowley, H., Varum, H., Pinho, R. and Sousa, R. [2014] "Evaluation of analytical methodologies used to derive vulnerability functions," Earthquake Engineering and Structural Dynamics, pp. 181-204.

Weitzman, M.L. [2001] "Gamma discounting," American Economic Review, 91(1), pp. 260-271.

Restrepo, F.C. [2008] "Tasa de descuento ambiental Gamma: una aplicación para Colombia," Lecturas de Economía, 69, pp. 143-162.

Edwards, G. [2016] "Estimación de la tasa social de descuento a largo plazo en el marco de los sistemas nacionales de inversión: aplicación al caso chileno," El Trimestre Económico, 83(329), pp. 99-125.

Castillo, J.G. and Zhangallimbay, D. [2022] "La tasa social de descuento en la evaluación de proyectos de inversión: una aplicación para el Ecuador," Revista CEPAL, 134, pp. 77-96.

United Nations Office for Disaster Risk Reduction (UNDRR) [2015] Global Risk Assessment Data, Methodology and Usage: Annex 1, UNDRR, Geneva, Switzerland.

World Bank Group (WBG) [2017] Country Disaster Risk Profiles: Technical Step-by-Step Guide to the CDRP Property (Building Stock) Model, World Bank Group, Washington, DC, USA.

[Example of conference reference]

Abrams, D.P. [1992] "Strength and behaviour of unreinforced masonry elements," *Proceedings of 10th World Conference on Earthquake Engineering*, Madrid, Spain.

[Example of dissertation / individual study / thesis reference]

Crowley, H. [2005] "An investigative study on the modelling of earthquake hazard for loss assessment," *Individual Study*, European School for Advanced Studies in Reduction of Seismic Risk (ROSE School), University of Pavia, Italy.

[Example of book reference]

Pinto, P.E., Giannini, R., Franchin, P. [2004] *Methods for Seismic Reliability Analysis of Structures*, IUSS Press, Pavia, Italy.

ICC [2003] *International Building Code*, International Code Council, USA.